Supplementary Information File

1. Methodology

1.1. Enzyme inhibition activity

1.1.1. Mushroom tyrosinase inhibitory assay

The mushroom tyrosinase (Sigma Chemical, USA) inhibition was performed following our previously reported methods [1]. In detail, 140 µL of phosphate buffer (20 mM, pH 6.8), 20 µL of mushroom tyrosinase (30 U/mL) and 20 µL of the inhibitor solution were placed in the wells of a 96-well micro plate. After pre-incubation for 10 min at room temperature, 20 µL of L-DOPA (3,4-dihydroxyphenylalanine, Sigma Chemical, USA) (0.85 mM) was added and the assay plate was further incubated at 25 °C for 20 min. Afterward the absorbance of dopachrome was measured at 475 nm using a micro plate reader (OPTI Max, Tunable). Kojic acid was used as a reference inhibitor and phosphate buffer was used as a negative control. The amount of inhibition by the test compounds was expressed as the percentage of concentration necessary to achieve 50% inhibition (IC_{50}). Each concentration was analyzed in three independent experiments. The IC_{50} values were determined by the data analysis and graphing software Origin 8.6, 64-bit.

The % of Inhibition of tyrosinase was calculated as following

$$\text{Inhibition (\%)} = [(B-S)/B] \times 100$$

Here, the B and S are the absorbance's for the blank and samples.

1.2. Kinetic analysis

A series of experiments were performed to calculate the inhibition kinetics of compounds **6P** by following the already reported method [1]. The compounds concentrations are: 0, 3.09, 6.18, 12.36 and 24.72 µM. Substrate L-DOPA concentration were between 0.5 to 3 mM in all kinetic

studies. Pre-incubation and measurement time was the same as discussed in mushroom tyrosinase inhibition assay protocol. Maximal initial velocity was determined from initial linear portion of absorbance up to five minutes after addition of enzyme at a 30 s interval. The inhibition type on the enzyme was assayed by Lineweaver-Burk plots of inverse of velocities ($1/V$) versus inverse of substrate concentration 1/[L-DOPA] mM^{-1}. The inhibition constant K_i was determined by Dixon plot of $1/V$ versus inhibitor concentrations.

1.3. Molecular docking study

Mushroom tyrosinase *Agaricus bisporus* crystal structure (PDB ID 2Y9X) has been frequently used by researchers as a model to investigate the inhibitory potential of compounds. The methodology for ligand and protein preparations and docking simulations were performed following our already reported methods [2-11].

1.4. MD simulation analysis

To analyze the protein ligand stability, a 100 ns MD simulation was performed. The complex was solvated in a periodic box with a 10 Å size containing the TIP3P water molecules [12]. Counter ions of Na^+ and Cl^- were introduced into the system to neutralize it. The system was minimized using the steepest decent method of 5000 steps following neutralization to remove steric conflicts. After minimization, the systems were prepared for the production run by equilibrating for 50,000 and 100,000 steps, respectively, at 310 K temperature at the NVT and NPT ensembles [13]. The simulation was conducted using Berendson thermostat and Parrinello-Rahman algorithms for maintaining constant temperature (310 K) and pressure (1 atm). By adjusting the time at τ P = 2.0 ps and τ T = 0.1 ps, the system was relaxed, and by applying the LINCS algorithm, the hydrogen atoms' bond lengths were kept at their ideal lengths [14], whereas Verlet computed the non-bonded interactions [15]. To compute the electrostatic interactions beyond the short-range limit, the particle mesh Ewald approach was used [16]. In x, y, and z dimensions, the periodic boundary conditions were imposed, and a production run was

conducted on the system. Every 10ps, the production run's trajectory was saved and examined using the R BIO3D package and gromacs commands [17] CHARMM36 forcefield and the Gromacs simulation program were used to execute the simulation [18].

1.5. QSAR analysis

The Canvas tool created a Structure-Activity Relationship (SAR) report to identify common scaffolds in bispyrimidines structures **(1P-8P)** utilized in this investigation. Bispyrimidines structures **(1P-8P)** in .mol file format used as input. The structure activity report requires the collection of input data (molecules, activity, preset scaffolds, and so on) as well as the recognition of common scaffolds. Canvas was used to perform the Quantitative Structure Activity Relationship (QSAR). The training set included all docked molecules. The QSAR model links activities with characteristics specific to each molecule in a test set. These features were assessed using a variety of molecular descriptors. Two stages are involved in QSAR research. Descriptors were created in the first phase to encode chemical structural information. A multiple linear regression (MLR) approach is employed in the second step to relate structural variation, as evaluated by descriptors, to variance in protein biological activity. Regression analysis was used to assess the findings dependability, employing inhibition activity as a dependent variable and description as a predictor factor. After confirming a good link of inhibitory activity with each unique description, QSAR models were generated [19].

2. Characterization Data

The spectroscopic data of bis-chalcones (**1C-6C & 8C**) are already reported in the literature [20-26]. Nevertheless, the spectral data of newly synthesized target compounds is given below.

3,3'-(1,4-Phenylene)bis(1-(3-bromo-5-chloro-2-hydroxyphenyl)prop-2-en-1-one) (7C)

Yellow solid; Yield: 89%; M.P: 271-273 °C; R_f (*n*-hexane: ethyl acetate, 3:1) = 0.87; UV λ_{max} (MeOH) = 266 nm; FTIR (KBr) cm^{-1}: 3449 (OH), 3030 (C-H), 1634 (C=O), 1562 (C=C), 1515

(aromatic C=C), 724 (Ar-Cl), 697 (Ar-Br); ^{1}H NMR (600 MHz, DMSO-d_6): δ 13.40 (bs, 2H, -OH), 8.52 (s, 2H, Ar-H), 8.10-8.05 (m, 4H, Ar-H and olefinic protons), 7.75-7.73 (m, 2H, olefinic protons), 7.68-7.64 (m, 4H, Ar-H); ^{13}C NMR (151 MHz, DMSO-d_6): δ 190.5, 156.7, 139.0, 138.4, 130.5, 130.4, 127.3, 127.2, 126.4, 125.5, 122.92, 122.89, 113.1, 79.7 (remaining carbons are isochronous); accurate mass (ESI) of $[M + H]^+$**:** Calculated for $C_{24}H_{15}Br_2Cl_2O_4$ 594.8714; found 594.8720.

6,6'-(1,4-Phenylene)bis(4-phenylpyrimidin-2-amine) (1P)

Yellow solid; Yield: 80%; M.P: 295-297 °C; R_f (*n*-hexane: ethyl acetate, 3:1) = 0.35; UV λ_{max} (MeOH) = 253 nm; FTIR (KBr) cm^{-1}: 3304 (NH_2), 3188 (N-H), 3060 (C-H), 1626 (C=N), 1541 (C=C), 1356 (C-N); ^{1}H NMR (600 MHz, DMSO-d_6): δ 8.40 (s, 4H, Ar-H), 8.26-8.24 (m, 4H, Ar-H), 7.82 (s, 2H, Ar-H), 7.56-7.52 (m, 6H, Ar-H), 6.83 (s, 4H, -NH_2); ^{13}C NMR (151 MHz, DMSO-d_6): δ 165.54, 164.60, 164.53, 139.56, 137.76, 131.00, 129.12, 127.69, 127.51, 102.56, 102.06 (remaining carbons are isochronous); accurate mass (ESI) of $[M + H]^+$**:** Calculated for $C_{26}H_{21}N_6$ 417.1827; found 417.1824.

6,6'-(1,4-Phenylene)bis(4-(4-iodophenyl)pyrimidin-2-amine) (2P)

Light Brown solid; Yield: 75%; M.P: > 340 °C; R_f (*n*-hexane: ethyl acetate, 3:1) = 0.80; UV λ_{max} (MeOH) = 260 nm; FTIR (KBr) cm^{-1}: 3367 (NH_2), 3189 (N-H), 3050 (C-H), 1567 (C=C), 1534 (C=N), 1363 (C-N); ^{1}H NMR (600 MHz, DMSO-d_6): δ 8.40 (s, 4H, Ar-H), 8.24 (dd, J = 12.0, 6.0 Hz, 4H, Ar-H), 7.85 (s, 2H, Ar-H), 7.77 (d, J = 12.0, 6.0 Hz, 4H, Ar-H), 6.85 (s, 4H, -NH_2); ^{13}C NMR (151 MHz, DMSO-d_6): δ 164.9, 164.5, 164.3, 139.5, 137.1, 132.2, 129.7, 127.8, 124.7, 102.4 (remaining carbons are isochronous); accurate mass (ESI) of $[M + H]^+$: Calculated for $C_{26}H_{19}I_2N_6$ 668.9761; found 668.9750.

6,6'-(1,4-Phenylene)bis(4-(4-fluorophenyl)pyrimidin-2-amine) (3P)

Yellow solid; Yield: 75%; M.P: 331-333 °C; R_f (*n*-hexane: ethyl acetate, 3:1) = 0.42; UV λ_{max} (MeOH) =264 nm; FTIR (KBr) cm^{-1}: 3202 (NH_2), 3189 (N-H), 3030 (C-H), 1631 (C=N), 1541 (C=C), 1355 (C-N), 1217 (C-F); ^1H NMR (600 MHz, DMSO-d_6): δ 8.35 (s, 4H, Ar-H), 8.31-8.29 (m, 4H, Ar-H), 7.79 (s, 2H, Ar-H), 7.36 (t, *J* = 12.0 Hz, 4H, Ar-H), 6.77 (s, 4H, -NH_2);^{13}C NMR (151 MHz, DMSO-d_6): δ 164.7, 164.4, 164.3, 163.3, 139.4, 134.0, 129.9, 129.8, 127.7, 116.1, 116.0, 102.4 (remaining carbons are isochronous); accurate mass (ESI) of $[M + H]^+$**:** Calculated for $C_{26}H_{19}F_2N_6$ 453.1639; found 453.1630.

6,6'-(1,4-Phenylene)bis(4-(*p*-tolyl)pyrimidin-2-amine) (4P)

Light brown solid; Yield: 75%; M.P: 312-314 °C; R_f (*n*-hexane: ethyl acetate, 3:1) = 0.56; UV λ_{max} (MeOH) = 262 nm; FTIR (KBr) cm^{-1}: 3483,3312 (NH_2), 3191, 1572, 789 (N-H), 2865 (C-CH_3), 3030 (C-H), 1623 (C=N), 1530 (C=C), 1360 (C-N); ^1H NMR (600 MHz, DMSO-d_6): δ 8.36 (s, 4H, Ar-H), 8.16 (d, *J* = 6.0 Hz, 4H, Ar-H), 7.77 (s, 2H, Ar-H), 7.36 (d, *J* = 6.0 Hz, 4H, Ar-H), 6.76 (s, 4H, -NH_2), 2.39 (s, 6H, -CH_3); ^{13}C NMR (151 MHz, DMSO-d_6): δ 165.4, 164.4, 164.4, 140.8, 139.5, 135.0, 129.7, 127.6, 127.4, 102.2, 21.4 (remaining carbons are isochronous); accurate mass (ESI) of $[M + H]^+$**:** Calculated for $C_{28}H_{25}N_6$ 445.2141; found 445.2138.

6,6'-(1,4-Phenylene)bis[4-(4-bromophenyl)pyrimidin-2-amine] (5P)

Light brown solid; Yield: 80%; M.P: 346-348 °C; R_f (*n*-hexane: ethyl acetate, 3:1) = 0.74; UV λ_{max} (MeOH) = 268 nm; FTIR (KBr) cm^{-1}: 3318 (NH_2), 3198 (N-H), 3020 (C-H), 1637 (C=N), 1569 (C=C), 1391 (C-N), 630 (Ar-Br); ^1H NMR (600 MHz, DMSO-d_6): δ 8.38 (s, 4H, Ar-H), 8.23 (dd, *J* = 12.0, 6.0 Hz, 4H, Ar-H), 7.84 (s, 2H, Ar-H), 7.76 (d, *J* = 12.0, 6.0 Hz, 4H, Ar-H), 6.86 (s, 4H, -NH_2); ^{13}C NMR (151 MHz, DMSO-d_6): δ 164.8, 164.4, 164.3, 139.4, 137.0, 132.1, 129.5, 127.7, 124.6, 102.4 (remaining carbons are isochronous); accurate mass (ESI) of $[M + H]^+$**:** Calculated for $C_{26}H_{19}Br_2N_6$ 573.0038; found 573.0040.

6,6'-(1,4-Phenylene)bis[4-(4-aminophenyl)pyrimidin-2-amine] (6P)

Yellow solid; Yield: 79%; M.P: 321-323 °C; R_f (*n*-hexane: ethyl acetate, 3:1) = 0.61; UV λ_{max} (MeOH) = 275 nm; FTIR (KBr) cm^{-1}: 3335 (NH_2), 3213 (N-H), 3030 (C-H), 1640 (C=N), 1597 (C=C), 1339 (C-N); ^1H NMR (600 MHz, DMSO-d_6): δ 7.95 (d, J = 12.0 Hz, 4H, Ar-H), 7.93 (s, 2H, Ar-H), 7.90 (s, 4H, Ar-H), 7.65 (s, 2H, -NH_2), 7.63 (s, 2H, -NH_2), 6.65 (d, J = 12.0 Hz, 4H, Ar-H), 6.19 (s, 4H, -NH_2); ^{13}C NMR (151 MHz, DMSO-d_6): δ 154.4, 141.2, 141.1, 137.1, 131.7, 129.5, 129.4, 129.3, 128.6, 128.4, 125.79, 125.74, 123.6, 113.2 (remaining carbons are isochronous); accurate mass (ESI) of $[M + H]^+$**:** Calculated for $C_{26}H_{23}N_8$ 447.2046; found 447.2049.

6,6'-(6,6'-(1,4-Phenylene)bis(2-aminopyrimidine-6,4-diyl))bis(2-bromo-4-chlorophenol) (7P)

Red solid; Yield: 83%; M.P: 319-321 °C; R_f (*n*-hexane: ethyl acetate, 3:1) = 0.45; UV λ_{max} (MeOH) = 266 nm; FTIR (KBr) cm^{-1}: 3441 (OH), 3360 (NH_2), 3168 (N-H), 3010 (C-H), 1643 (C=N), 1543 (C=C), 1384 (C-N), 773 (Ar-Cl), 697 (Ar-Br); ^1H NMR (600 MHz, DMSO-d_6): δ 7.84 (d, *J* = 6.0 Hz, 2H, Ar-H), 7.67 (s, 4H, Ar-H), 7.45-7.41 (m, 4H, Ar-H), 7.34-7.32 (m, 4H, -NH_2), 7.30 (d, *J* = 6.0 Hz, 2H, Ar-H), 5.48 (bs, 2H, -OH); ^{13}C NMR (151 MHz, DMSO-d_6): δ 168.6, 168.3, 160.1, 141.8, 137.5, 137.4, 135.0, 131.2, 129.5, 128.8, 128.6, 128.6, 127.4, 125.8, 123.2, 110.2, 62.4 (remaining carbons are isochronous); accurate mass (ESI) of $[M + H]^+$**:** Calculated for $C_{26}H_{17}Br_2Cl_2N_6O_2$ 672.9157; found 672.9164.

4,4'-[6,6'-(1,4-Phenylene)bis(2-aminopyrimidine-6,4-diyl))diphenol] (8P)

Brown solid; Yield: 79%; M.P: 235-237 °C; R_f (*n*-hexane: ethyl acetate, 3:1) = 0.42; UV λ_{max} (MeOH) = 268 nm; FTIR (KBr) cm^{-1}: 3400 (OH), 3370 (NH_2), 3186 (N-H), 3020 (C-H), 1610 (C=N), 1541 (C=C), 1381 (C-N); ^1H NMR (600 MHz, DMSO-d_6): δ 7.84 (d, *J* = 12.0 Hz, 2H, Ar-H), 7.77 (d, *J* = 12.0 Hz, 4H, Ar-H), 7.62-7.57 (m, 2H, Ar-H), 7.45 (d, *J* = 12.0 Hz, 4H, Ar-H), δ 7.30 (d, *J* = 12.0 Hz, 2H, Ar-H), 7.08-6.99 (m, 4H, -NH_2), 5.52 (bs, 1H, -OH), 5.42 (bs,

1H, -OH); ^{13}C NMR (151 MHz, DMSO-d_6): δ 168.7, 168.6, 140.2, 131.6, 131.3, 130.4, 130.0, 129.7, 129.5, 128.8, 128.5, 127.5, 126.0, 122.7 (remaining carbons are isochronous); accurate mass (ESI) of $[M + H]^+$: Calculated for $C_{26}H_{21}N_6O_2$ 449.1726; found 449.1718.

References

1. Z. Ashraf, M. Rafiq, S.-Y. Seo, K. S. Kwon and M. M. Babar, *European Journal of Medicinal Chemistry*, 2015, **98**, 203-211.
2. E. U. Mughal, J. Ashraf, E. M. Hussein, Y. Nazir, A. S. Alwuthaynani, N. Naeem, A. Sadiq, R. I. Alsantali and S. A. Ahmed, *ACS omega*, 2022, **7**, 17444-17461.
3. Y. Nazir, A. Saeed, M. Rafiq, S. Afzal, A. Ali, M. Latif, J. Zuegg, W. M. Hussein, C. Fercher and R. T. Barnard, *Bioorganic & Medicinal Chemistry Letters*, 2020, **30**, 126722.
4. Y. Nazir, H. Rafique, N. Kausar, Q. Abbas, Z. Ashraf, P. Rachtanapun, K. Jantanasakulwong and W. Ruksiriwanich, *Molecules*, 2021, **26**, 2477.
5. Y. Nazir, H. Rafique, S. Roshan, S. Shamas, Z. Ashraf, M. Rafiq, T. Tahir, Z.-U.-R. Qureshi, A. Aslam and M. H. H. B. Asad, *BioMed Research International*, 2022, **2022**, 1040693.
6. M. Rafiq, Y. Nazir, Z. Ashraf, H. Rafique, S. Afzal, A. Mumtaz, M. Hassan, A. Ali, K. Afzal and M. R. Yousuf, *Journal of enzyme inhibition and medicinal chemistry*, 2019, **34**, 1562-1572.
7. N. A. Alshaye, E. U. Mughal, E. B. Elkaeed, Z. Ashraf, S. Kehili, Y. Nazir, N. Naeem, N. Abdul Majeed and A. Sadiq, *Journal of Biomolecular Structure and Dynamics*, 2023, **41**, 8307-8322.
8. M. M. Al-Rooqi, A. Sadiq, R. J. Obaid, Z. Ashraf, Y. Nazir, R. S. Jassas, N. Naeem, M. A. Alsharif, S. W. A. Shah and Z. Moussa, *ACS omega*, 2023, **8**, 17195-17208.

9. R. I. Alsantali, E. U. Mughal, N. Naeem, M. A. Alsharif, A. Sadiq, A. Ali, R. S. Jassas, Q. Javed, A. Javid and S. H. Sumrra, *Journal of Molecular Structure*, 2022, **1251**, 131933.

10. J. Ashraf, E. U. Mughal, R. I. Alsantali, R. J. Obaid, A. Sadiq, N. Naeem, A. Ali, A. Massadaq, Q. Javed and A. Javid, *Bioorganic & Medicinal Chemistry*, 2021, **35**, 116057.

11. J. Ashraf, E. U. Mughal, A. Sadiq, M. Bibi, N. Naeem, A. Ali, A. Massadaq, N. Fatima, A. Javid and M. N. Zafar, *Journal of Biomolecular Structure and Dynamics*, 2021, **39**, 7107-7122.

12. W. Jorgensen and J. J. J. C. P. Chandrasekhar, 1983, **79**, 926.

13. K. A. Qureshi, I. Al Nasr, W. S. Koko, T. A. Khan, M. Q. Fatmi, M. Imtiaz, R. A. Khan, H. A. Mohammed, M. Jaremko and A.-H. J. A. Emwas, 2021, **10**, 887.

14. B. Hess, H. Bekker, H. J. Berendsen and J. G. J. J. o. c. c. Fraaije, 1997, **18**, 1463-1472.

15. H. Grubmüller, H. Heller, A. Windemuth and K. J. M. S. Schulten, 1991, **6**, 121-142.

16. U. Essmann, L. Perera, M. L. Berkowitz, T. Darden, H. Lee and L. G. J. T. J. o. c. p. Pedersen, 1995, **103**, 8577-8593.

17. B. J. Grant, L. Skjærven and X. Q. J. P. S. Yao, 2021, **30**, 20-30.

18. J. Huang and A. D. J. J. o. c. c. MacKerell Jr, 2013, **34**, 2135-2145.

19. E. U. Mughal, S. Amjid, A. Sadiq, N. Naeem, Y. Nazir, H. Alrafai, A. A. Hassan, S. Y. Al-Nami, A. A. Abdel Hafez and S. W. Ali Shah, *Journal of Biomolecular Structure and Dynamics*, 2024, **42**, 244-260.

20. A. F. Abbas, *Synthesis*, 2015, **7**.

21. H. C. Kwong, A. J. Sim, C. Kumar, C. K. Quah, S. Chantrapromma, S. Naveen and I. Warad, *Acta Crystallographica Section E: Crystallographic Communications*, 2018, **74**, 835-839.

22. B. Jiang, F. Han, M.-H. Lü, Z.-P. Wang, W. Liu, Y.-X. Zhang, J. Xu and R.-J. Li, *European Journal of Medicinal Chemistry*, 2022, **239**, 114529.

23. C. Kumar, C. K. Quah, S. Chandraju, N. Lokanath, S. Naveen and M. Abdoh, *IUCrData*, 2017, **2**, x170238.

24. S. Kumar, B. Narasimhan, S. M. Lim, K. Ramasamy, V. Mani and S. A. Shah, *Mini Reviews in Medicinal Chemistry*, 2019, **19**, 609-621.

25. A. A. Al-Khalaf, A. F. Abbas and H. S. Al-Lami, *Basrah Journal of Sciences*, 2022, **40**, 437-464.

26. Y. Wang, L. Li, T. Ma, X. Cheng and D. Liu, *Anti-Cancer Agents in Medicinal Chemistry (Formerly Current Medicinal Chemistry-Anti-Cancer Agents)*, 2022, **22**, 2116-2124.

UV Spectra of All the Newly Synthesized Target Compounds

UV Spectrum of Compound 7C

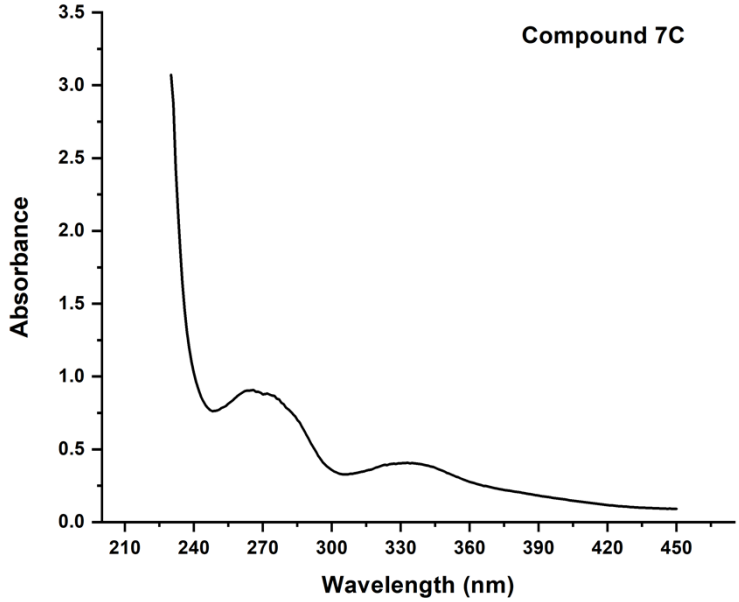

UV Spectrum of Compound 1P

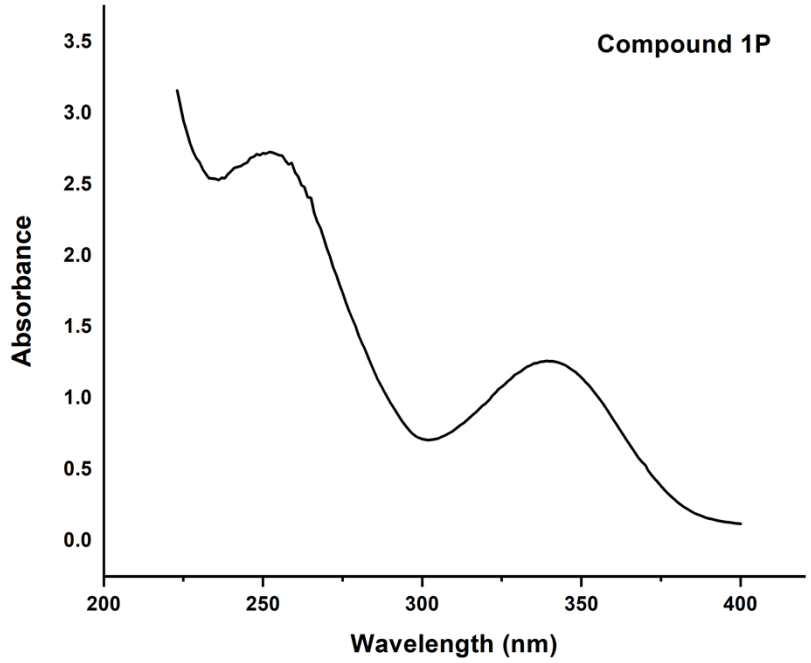

UV Spectrum of Compound 2P

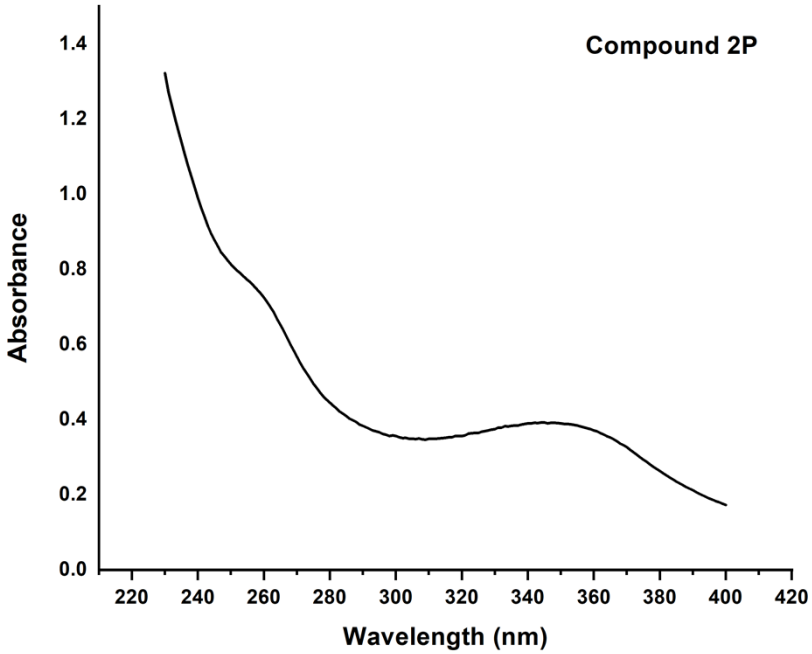

UV Spectrum of Compound 3P

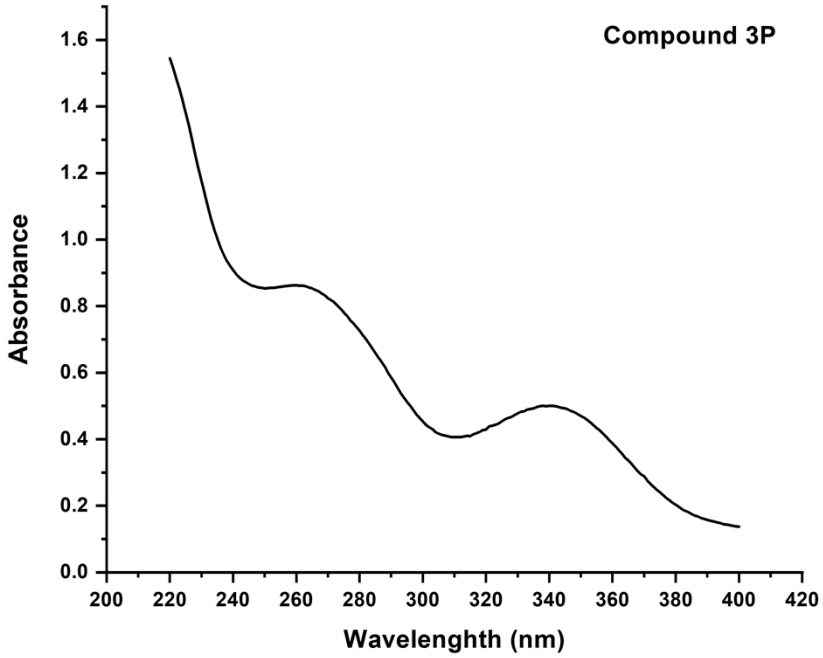

UV Spectrum of Compound 4P

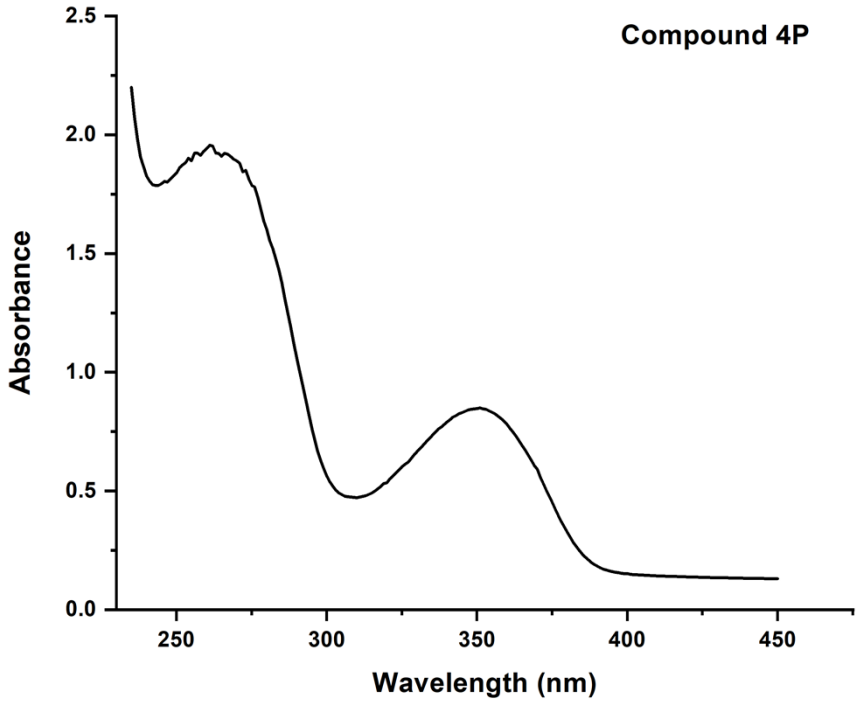

UV Spectrum of Compound 5P

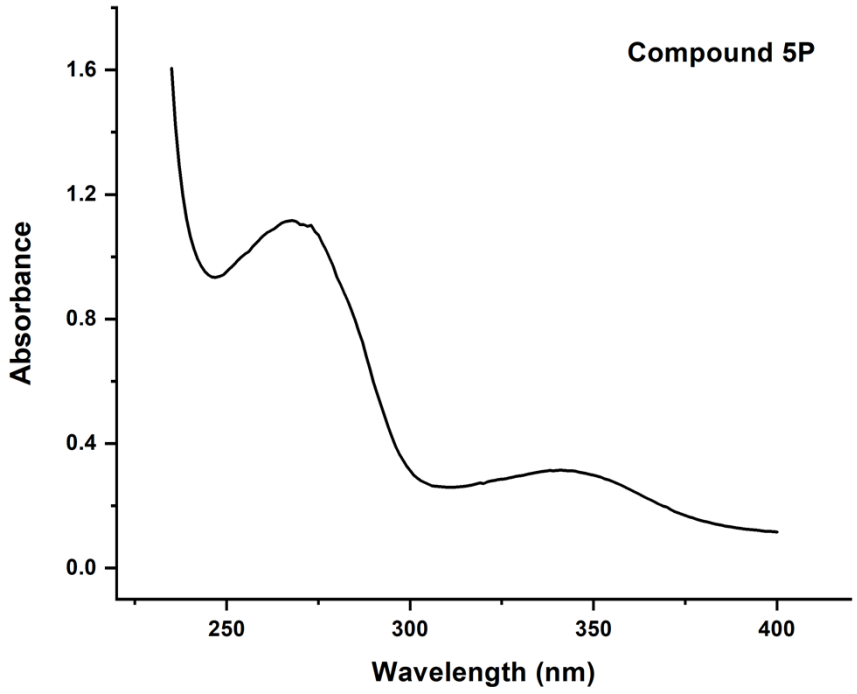

UV Spectrum of Compound 6P

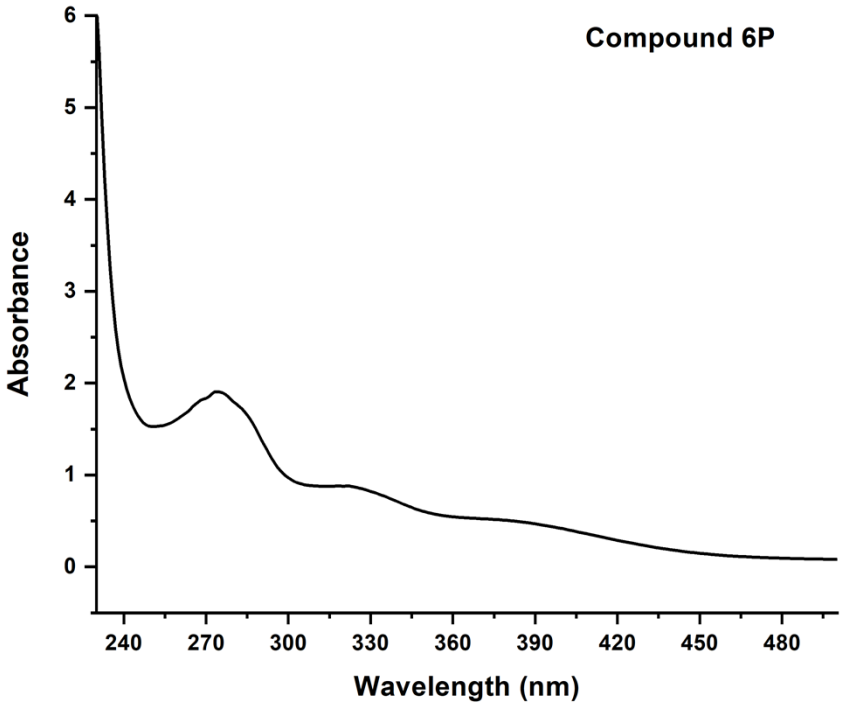

UV Spectrum of Compound 7P

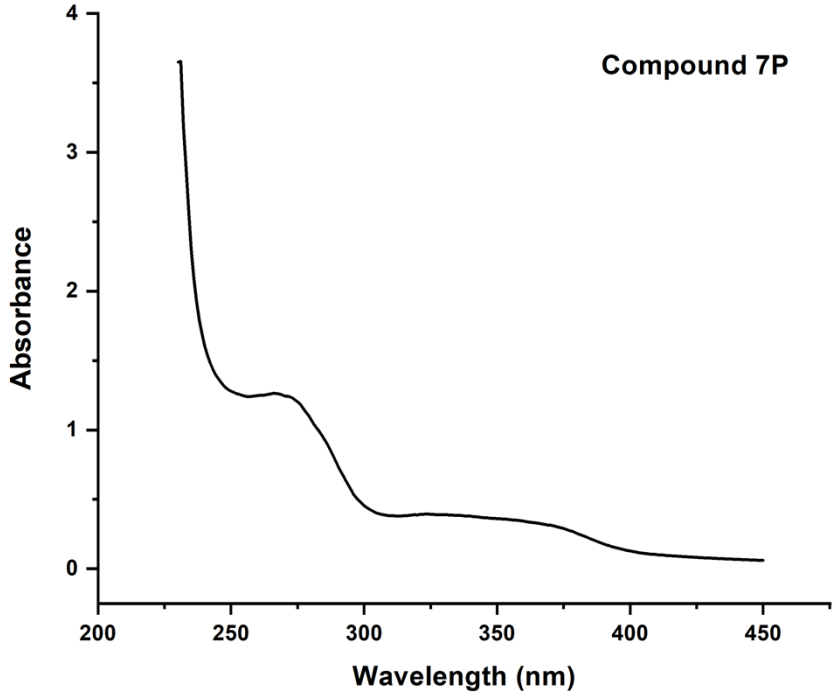

UV Spectrum of Compound 8P

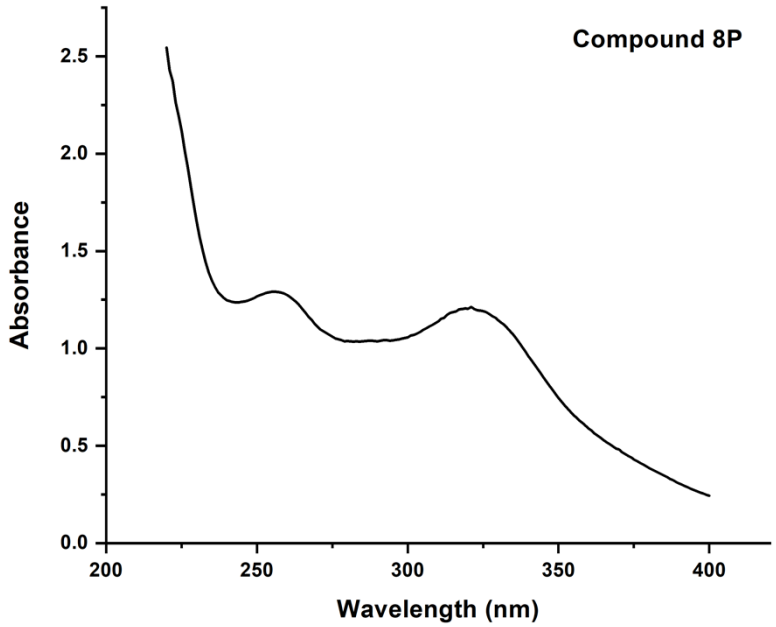

FTIR Spectra of All the Newly Synthesized Target Compounds

FTIR Spectrum of Compound 7C

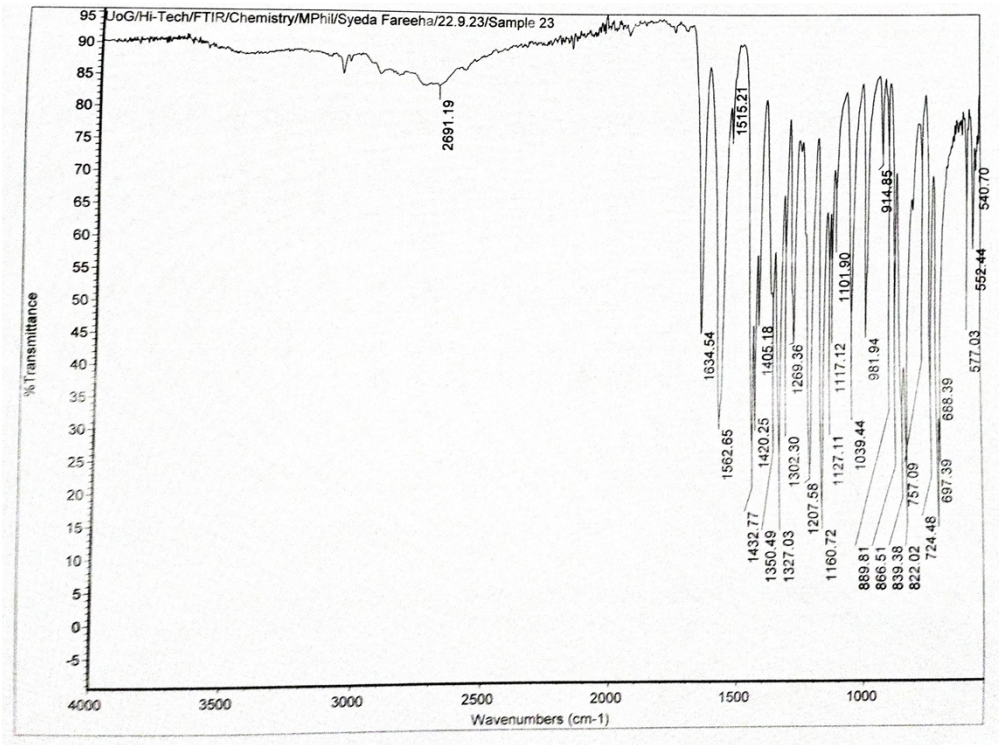

FTIR Spectrum of Compound 1P

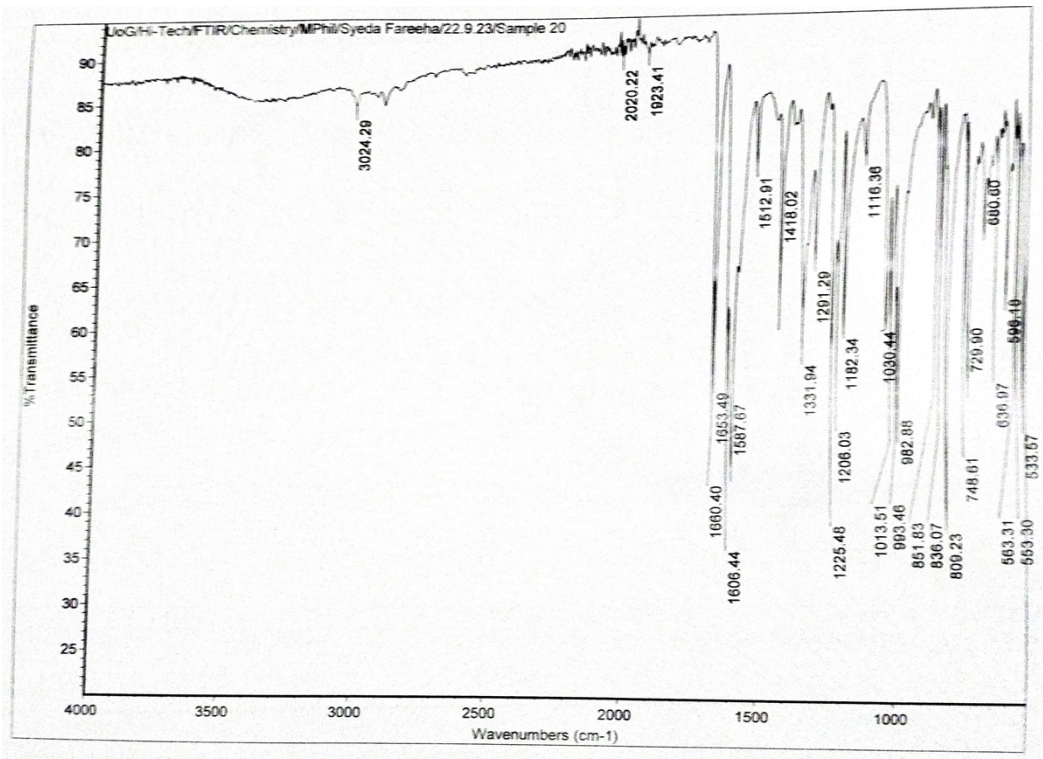

FTIR Spectrum of Compound 2P

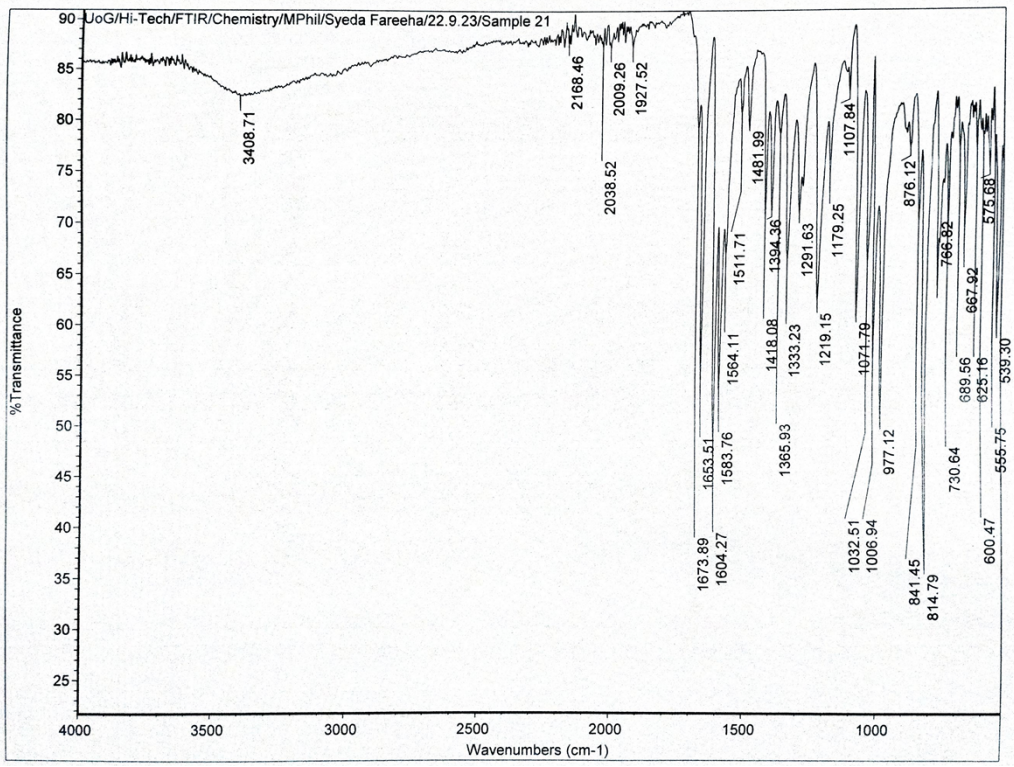

FTIR Spectrum of Compound 3P

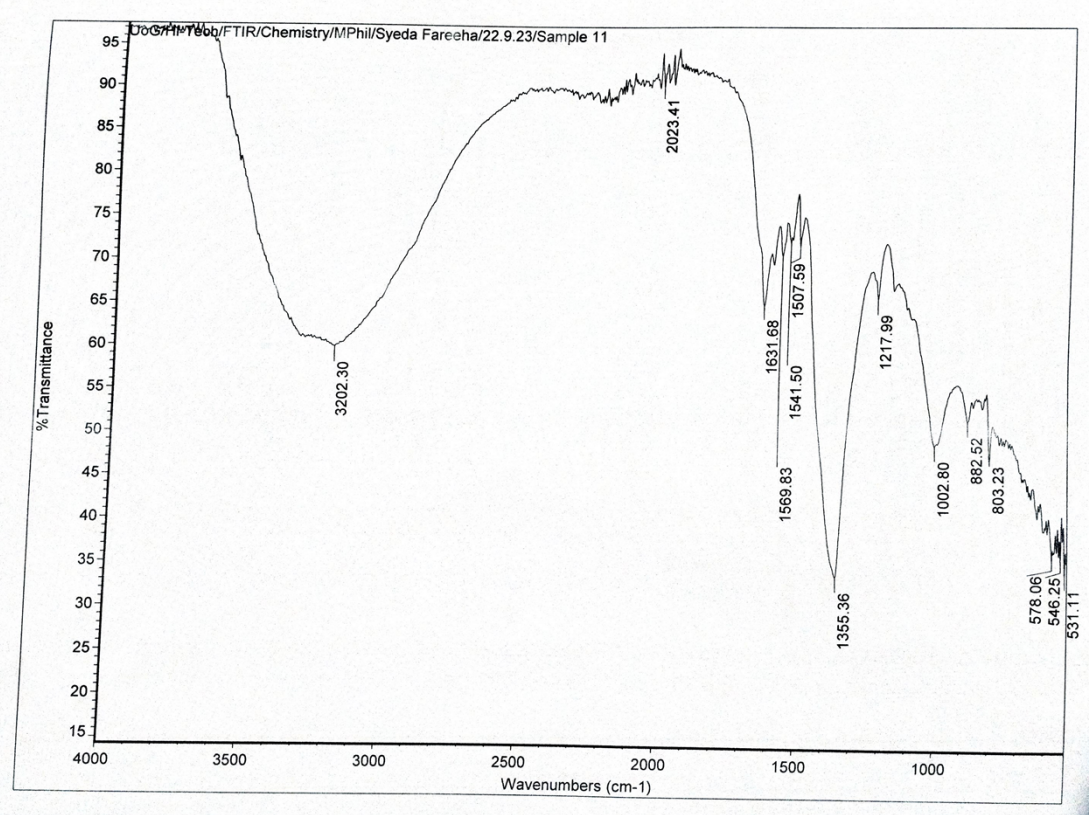

FTIR Spectrum of Compound 4P

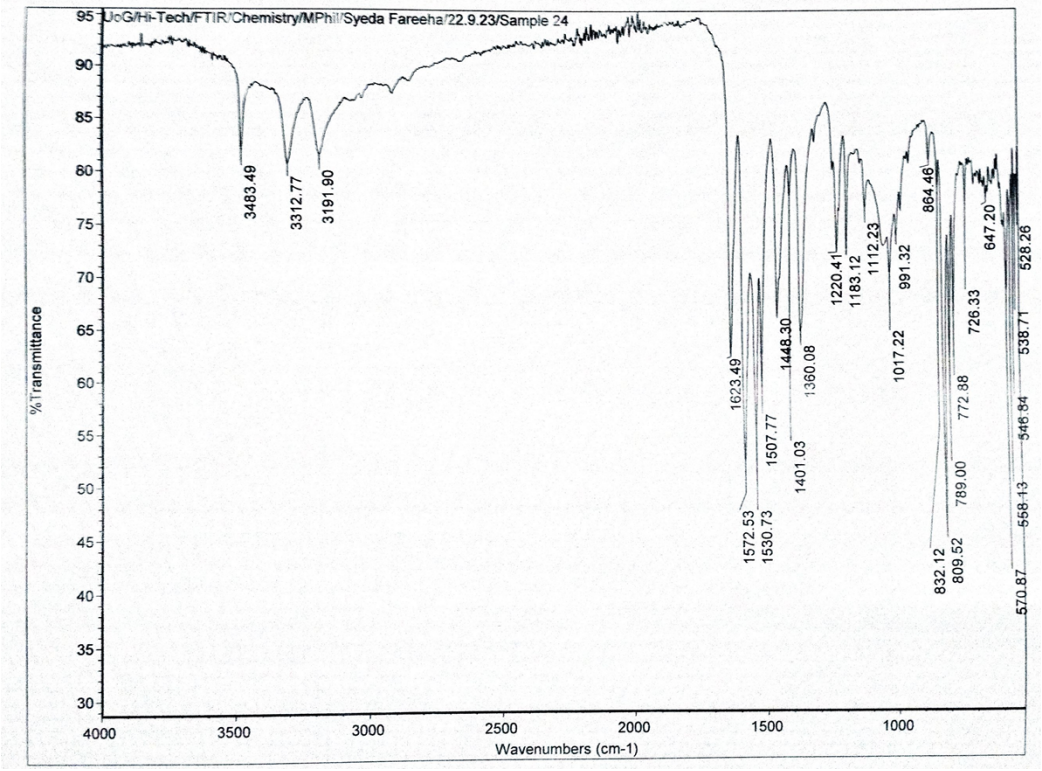

FTIR Spectrum of Compound 5P

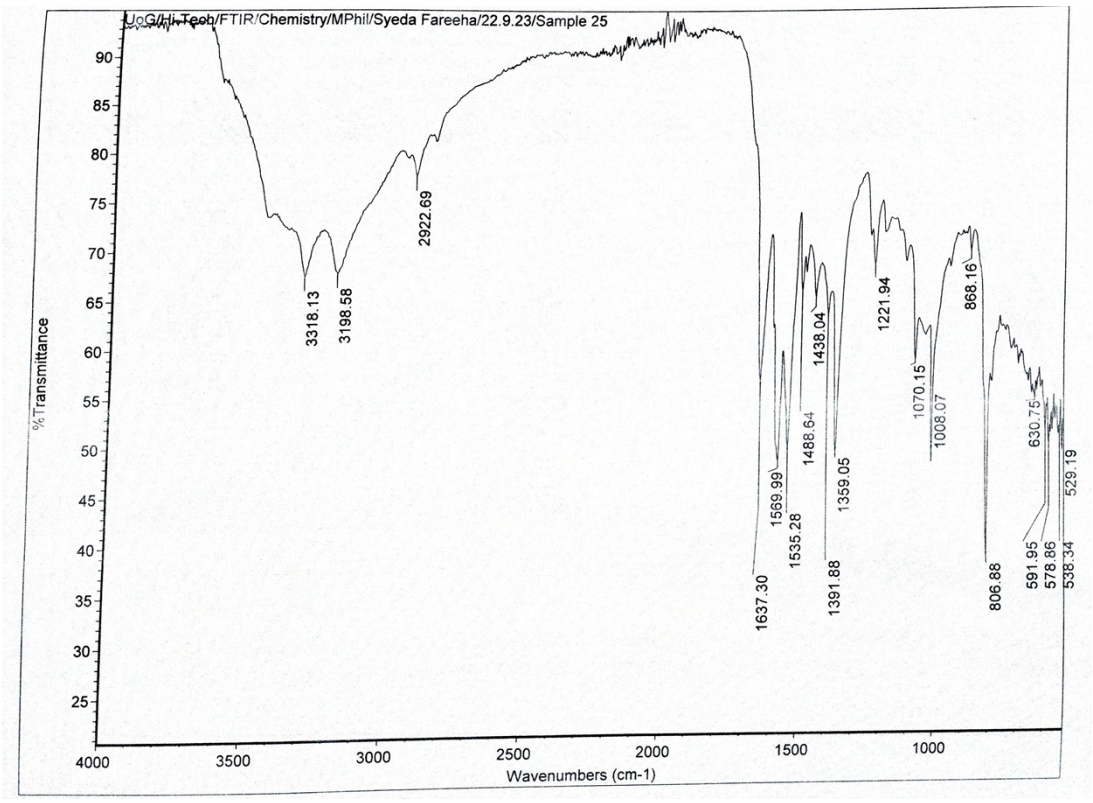

FTIR Spectrum of Compound 6P

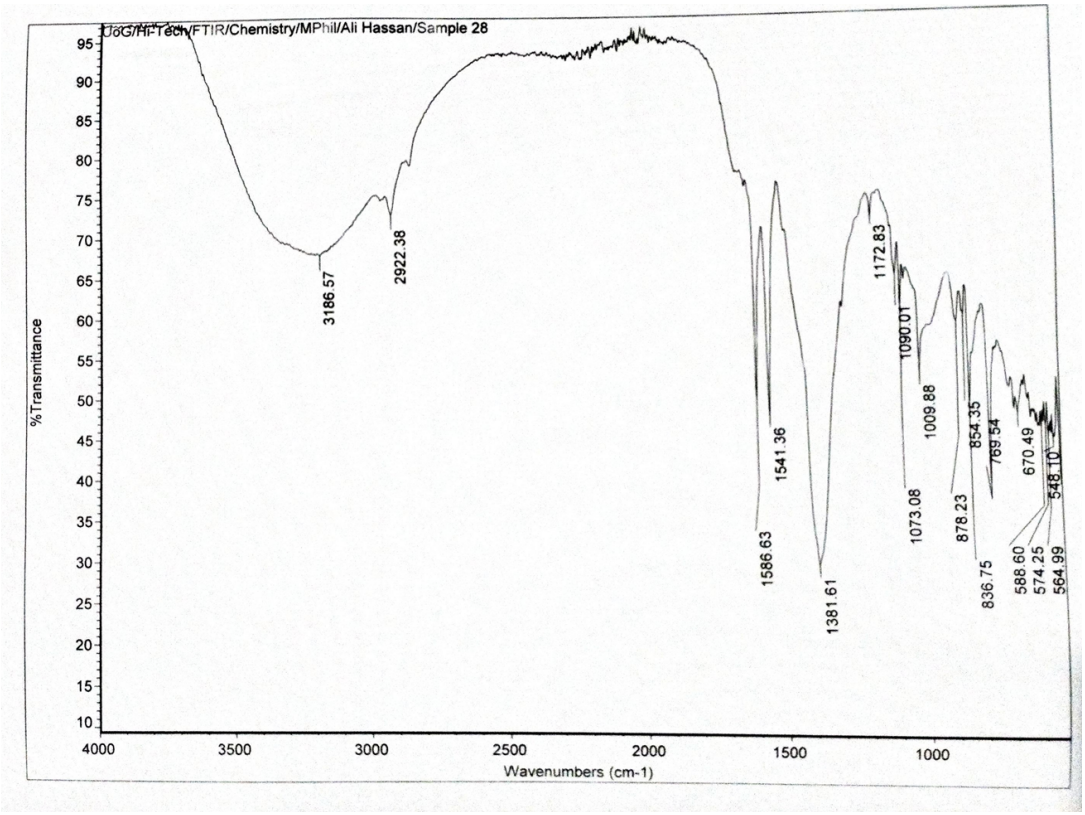

FTIR Spectrum of Compound 7P

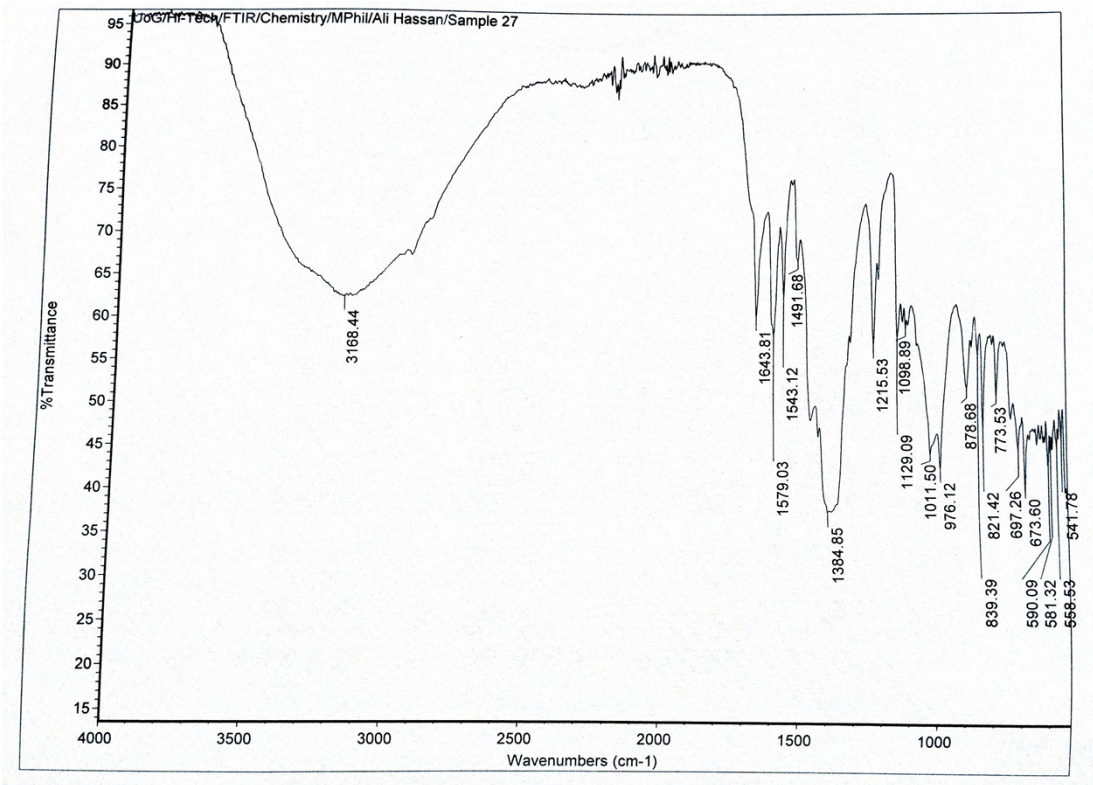

FTIR Spectrum of Compound 8P

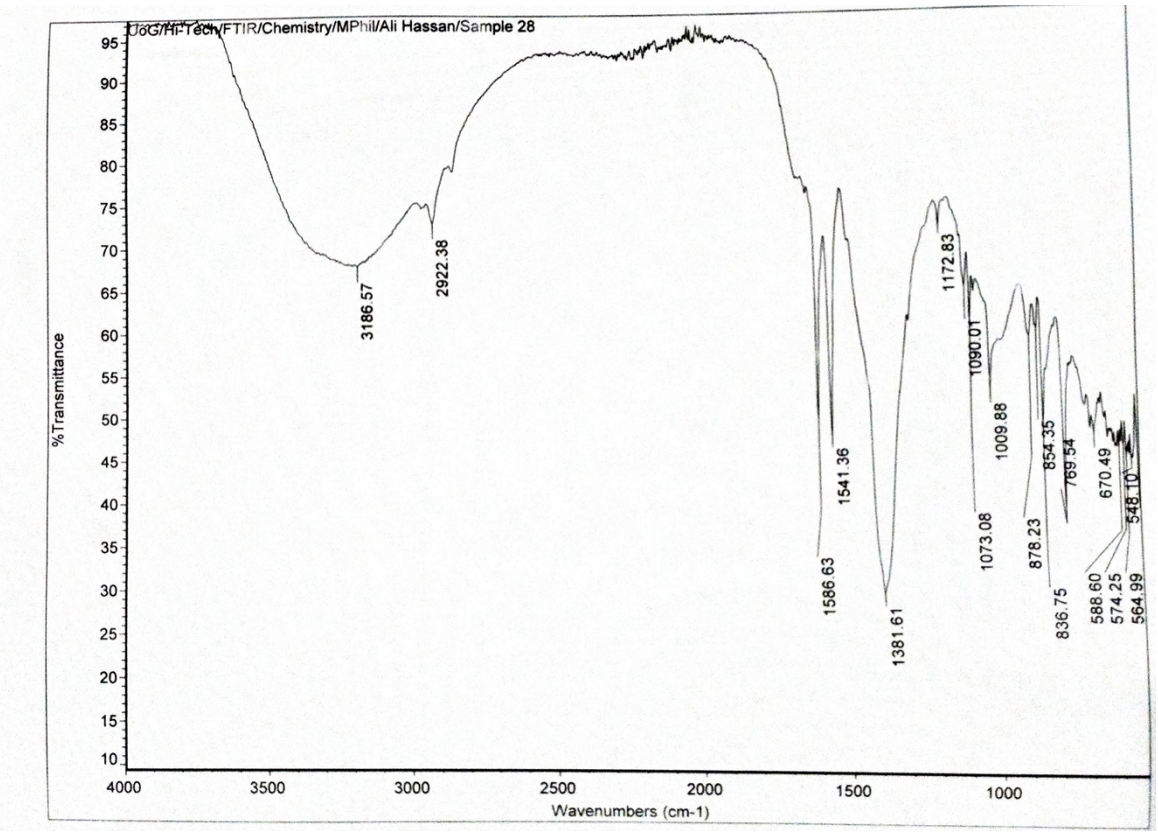
UoG/Hi-Tech/FTIR/Chemistry/MPhil/Ali Hassan/Sample 28
%Transmittance
Wavenumbers (cm-1)
3186.57
2922.38
1586.63
1541.36
1381.61
1172.83
1090.01
1073.08
1009.88
878.23
854.35
836.75
769.54
670.49
588.60
574.25
564.99
548.10

NMR Spectra of All the Newly Synthesized Target Compounds

^{1}H-NMR Spectrum (600 MHz, DMSO-d_6) of Compound 7C

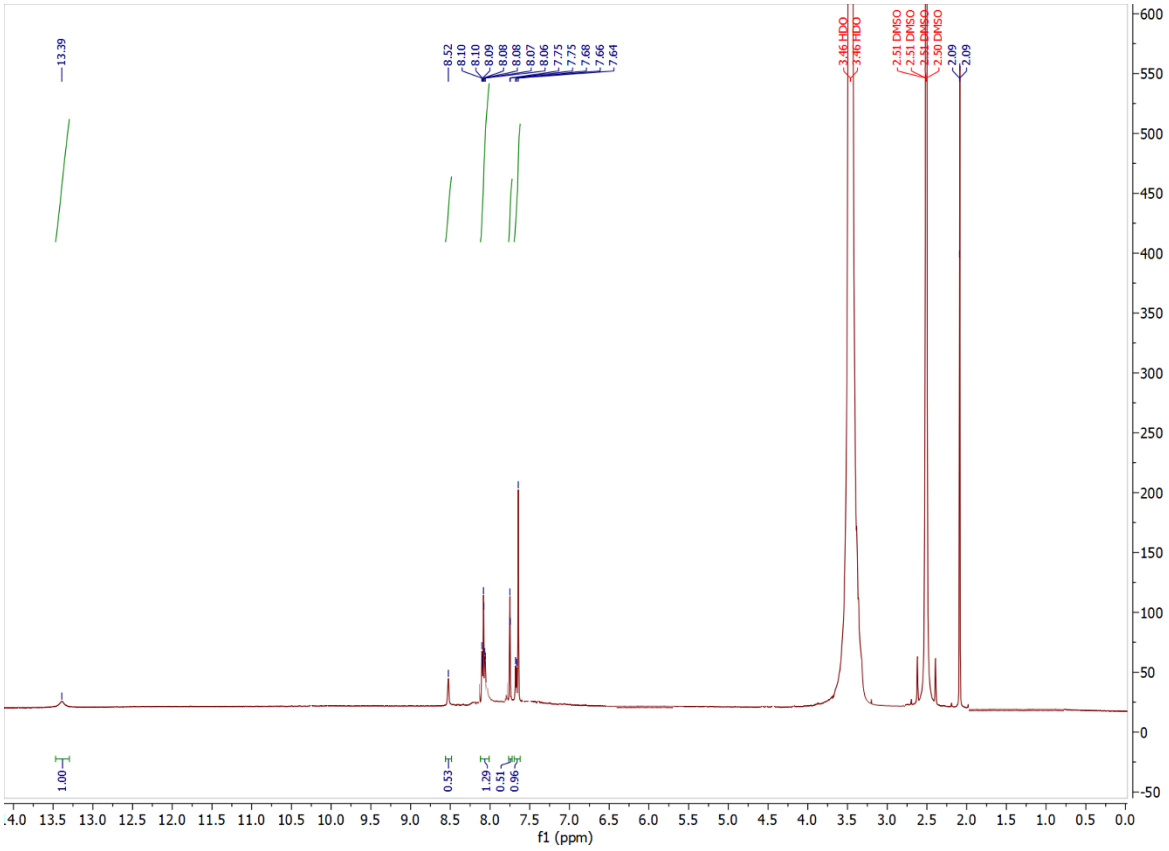

^{13}C-NMR Spectrum (151 MHz, DMSO-d_6) of Compound 7C

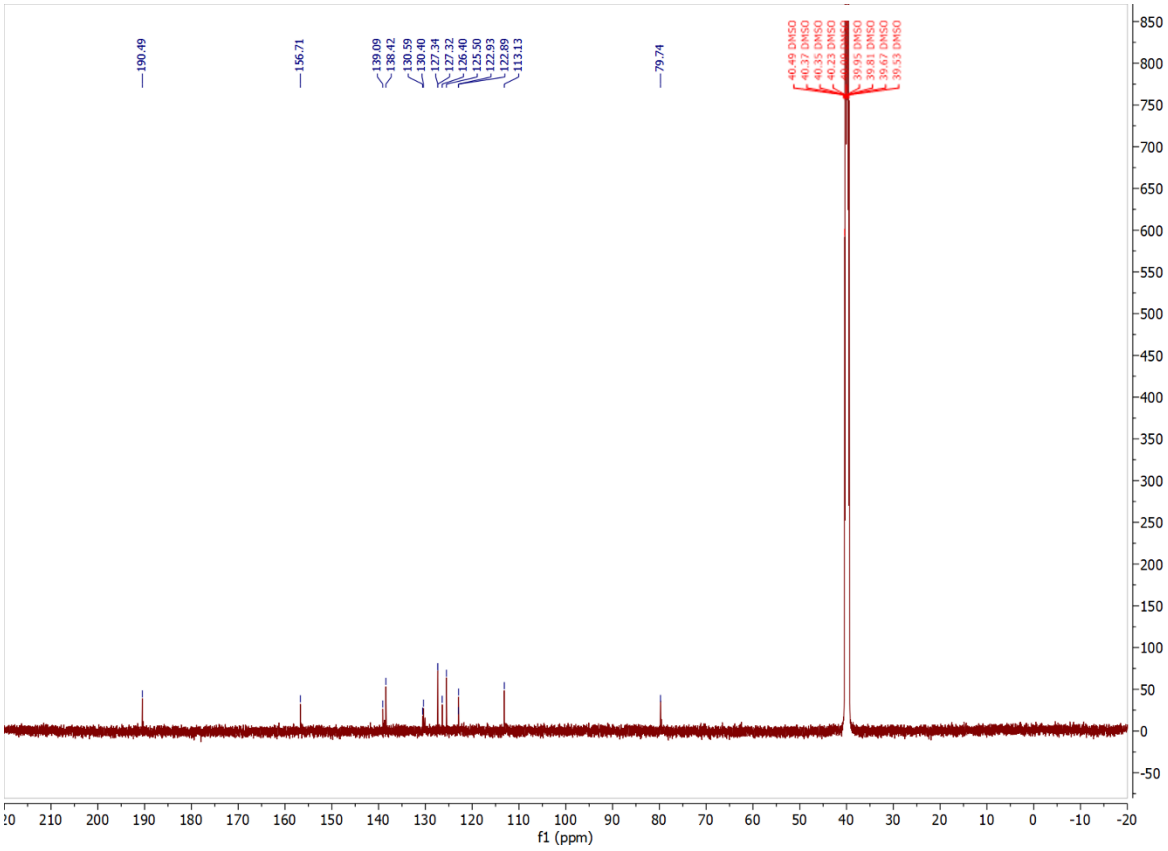

DEPT NMR Spectrum of Compound 7C

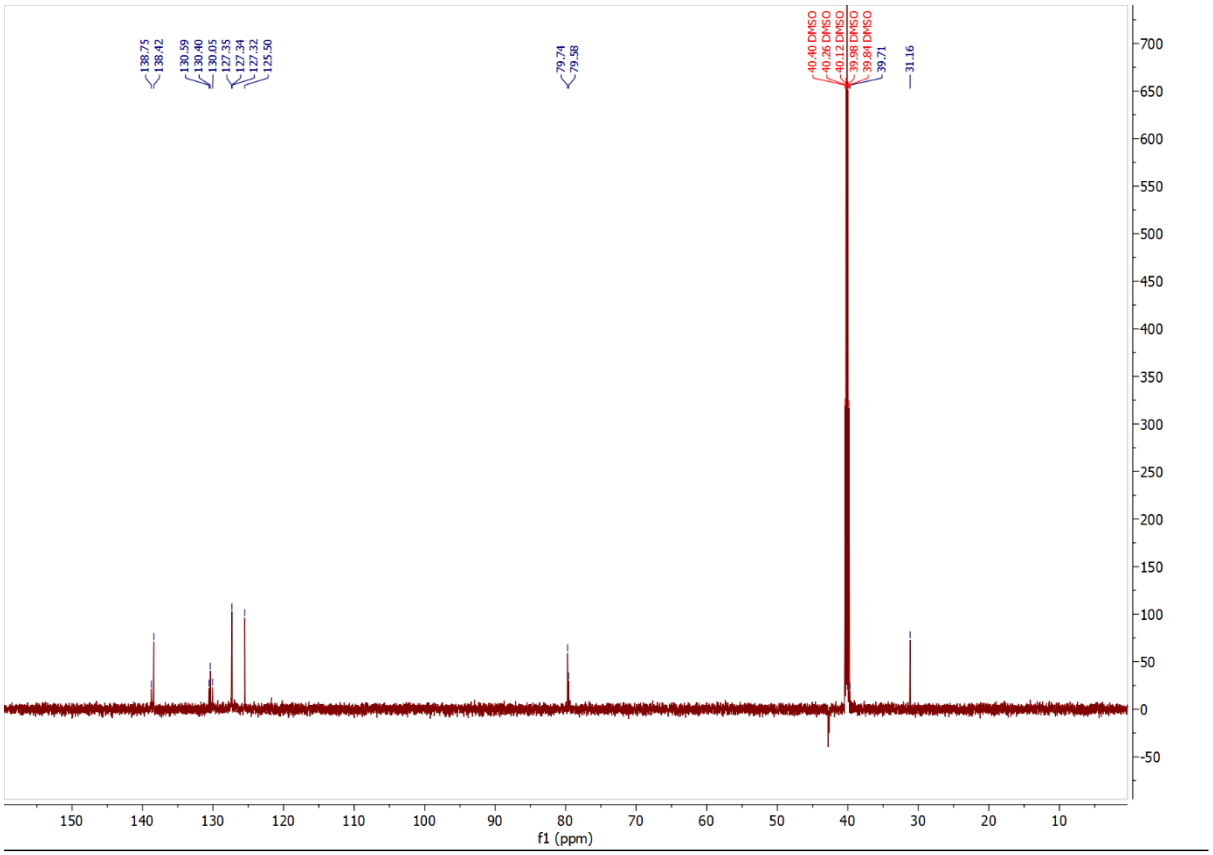

^{1}H-NMR Spectrum (600 MHz, DMSO-d_6) of Compound 1P

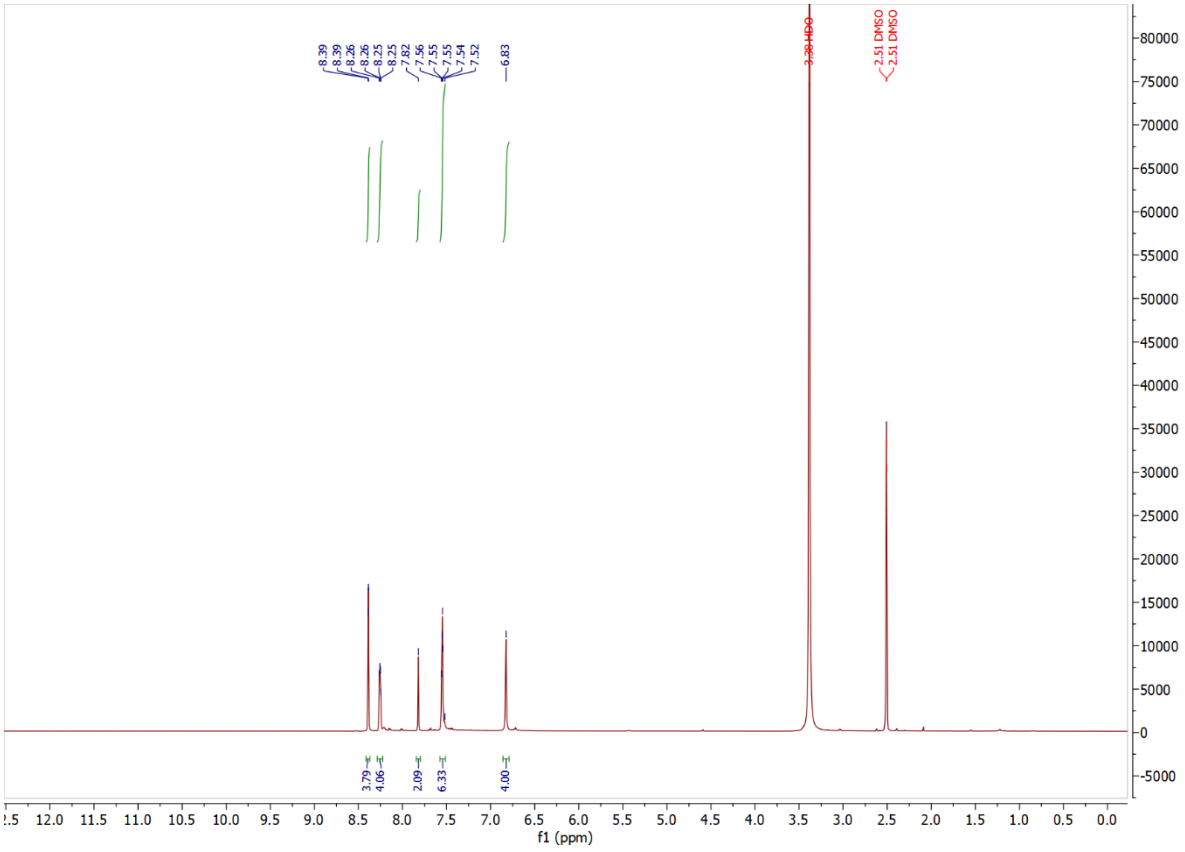

^{13}C-NMR Spectrum (151 MHz, DMSO-d_6) of Compound 1P

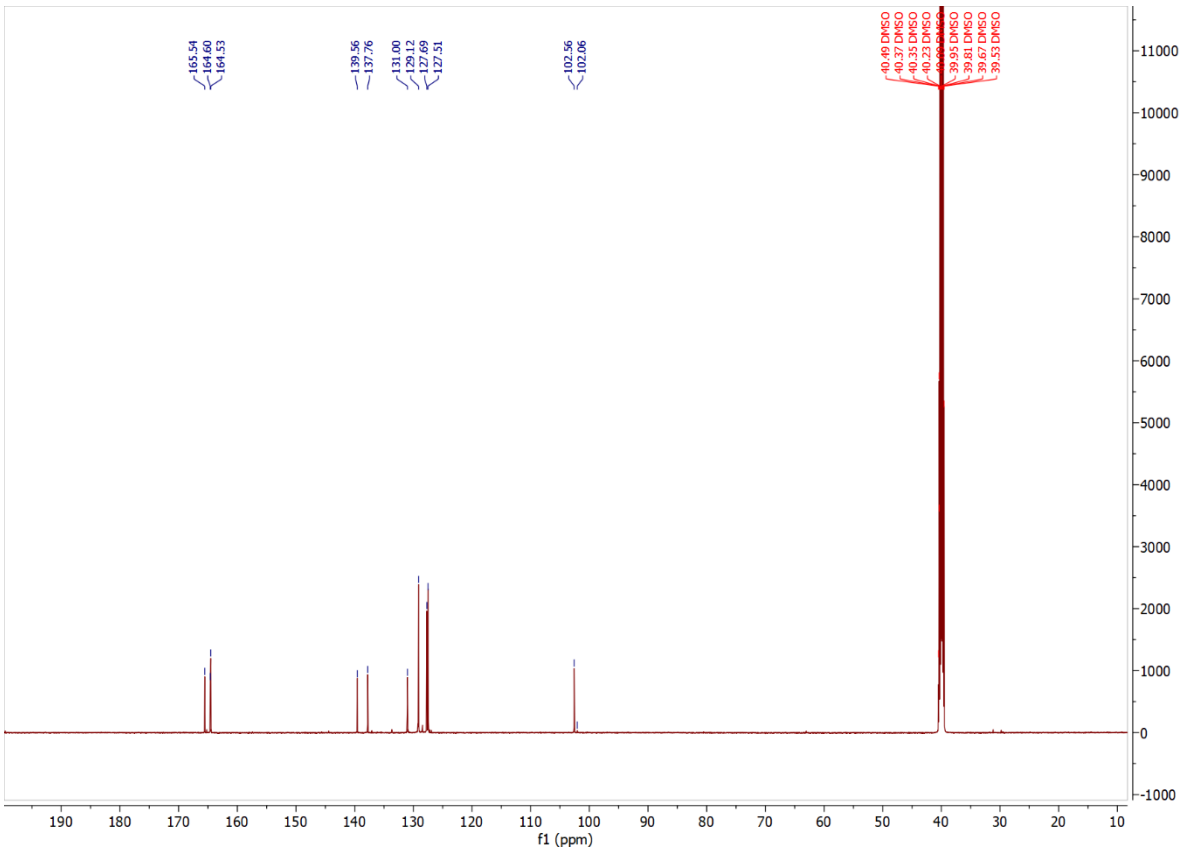

DEPT NMR Spectrum of Compound 1P

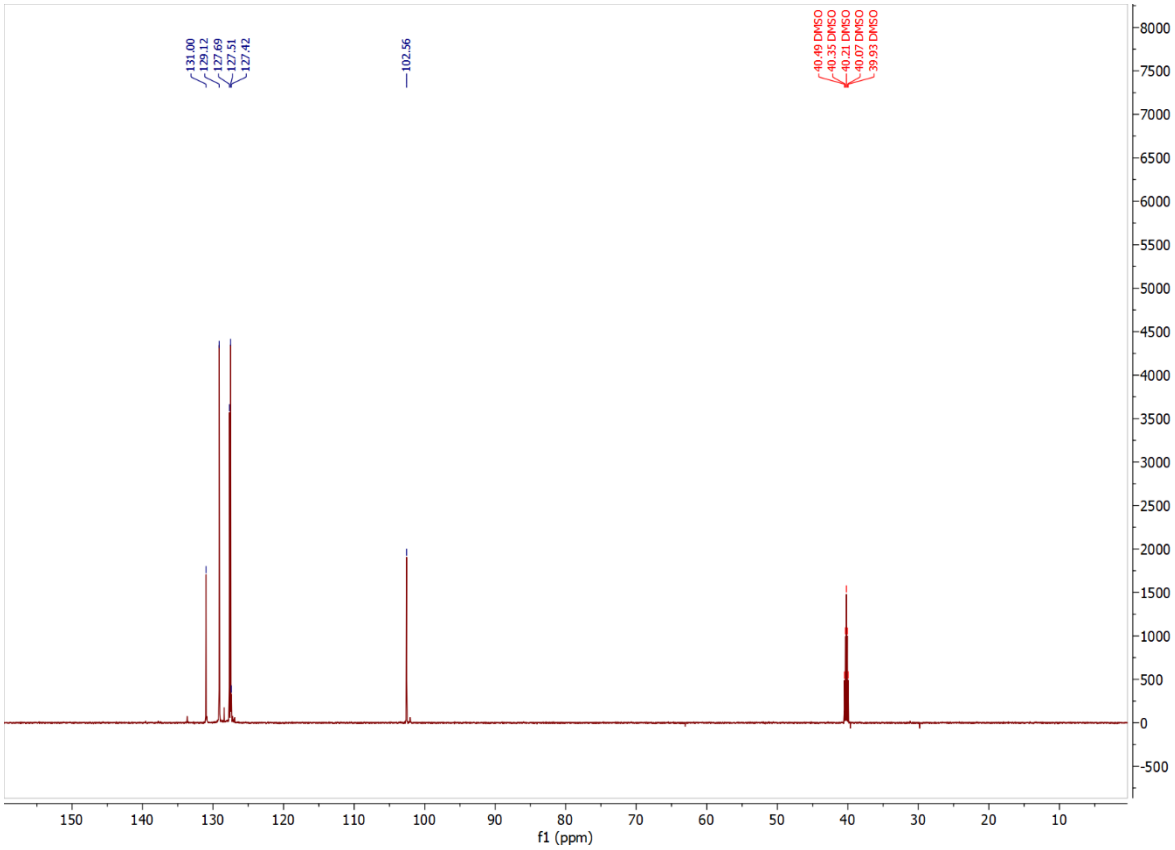

^{1}H-NMR Spectrum (600 MHz, DMSO-d_6) of Compound 2P

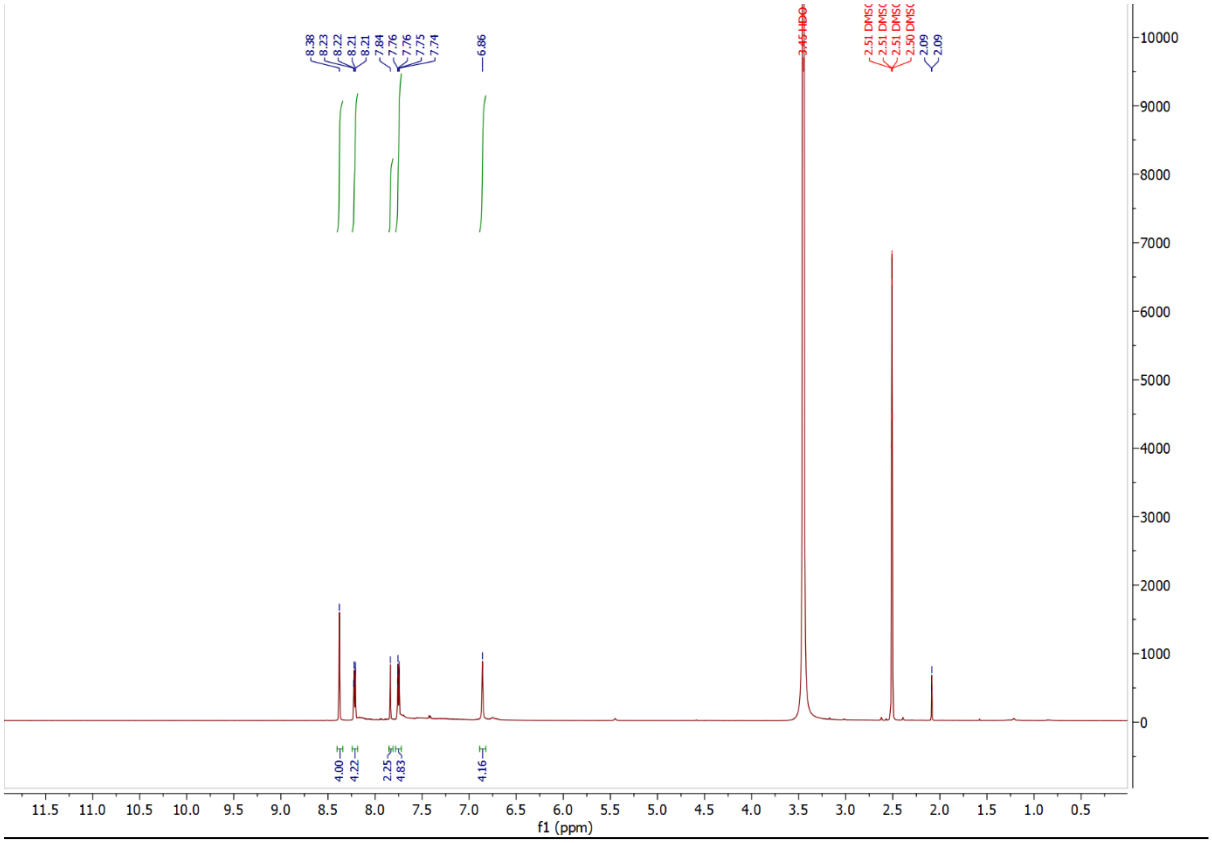

^{13}C-NMR Spectrum (151 MHz, DMSO-d_6) of Compound 2P

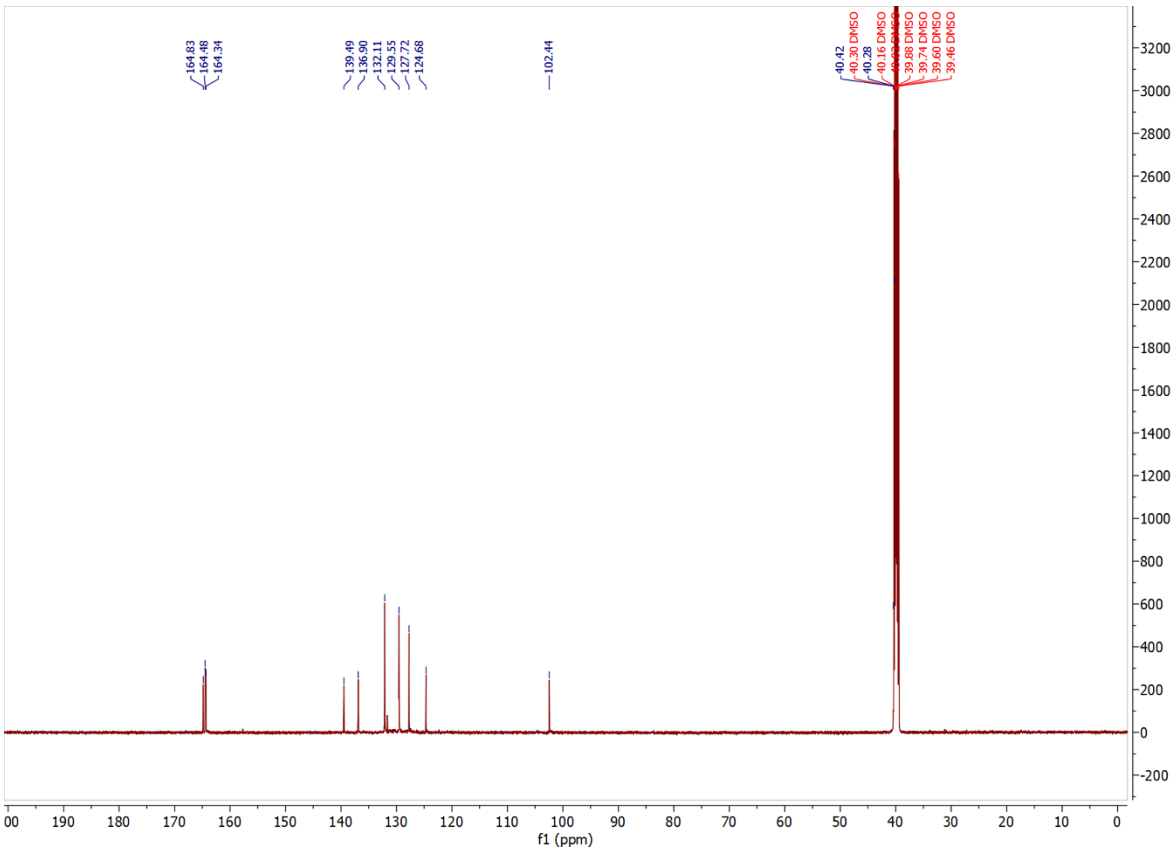

DEPT NMR Spectrum of Compound 2P

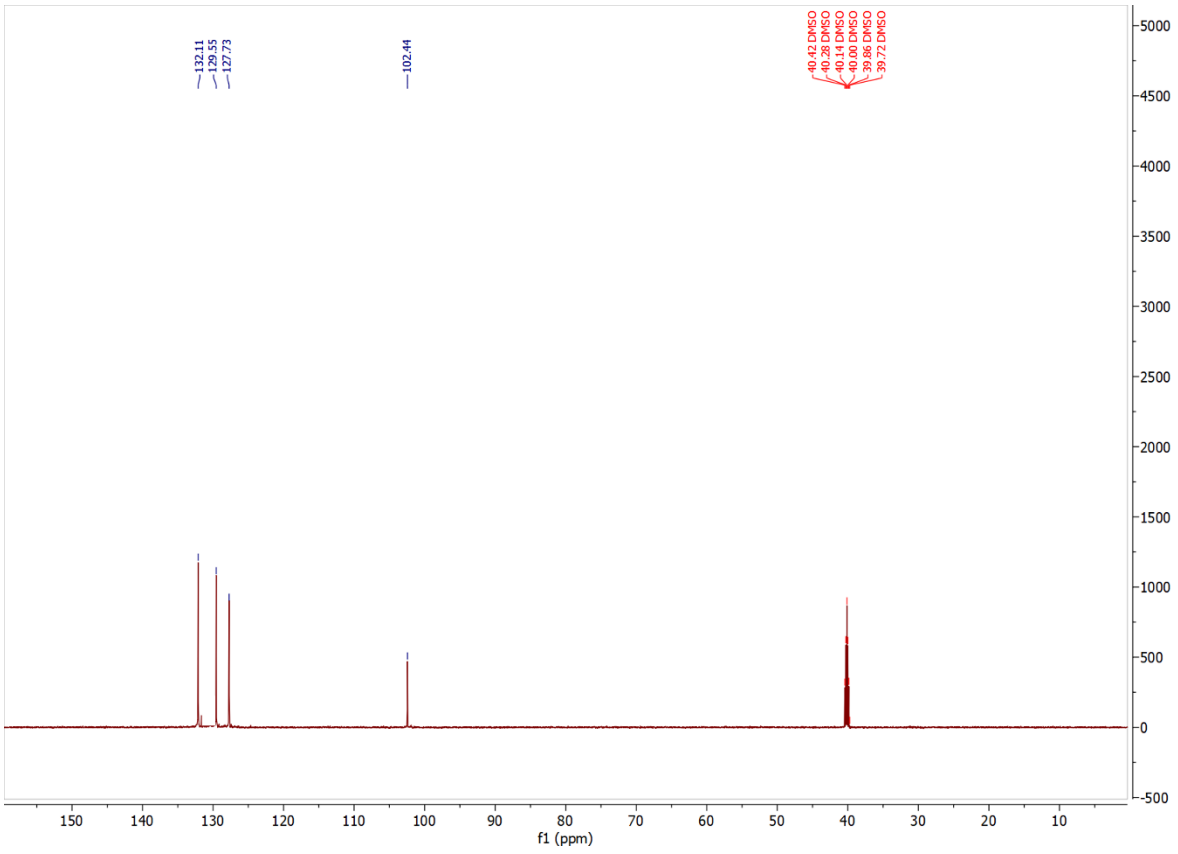

^{1}H-NMR Spectrum (600 MHz, DMSO-d_6) of Compound 3P

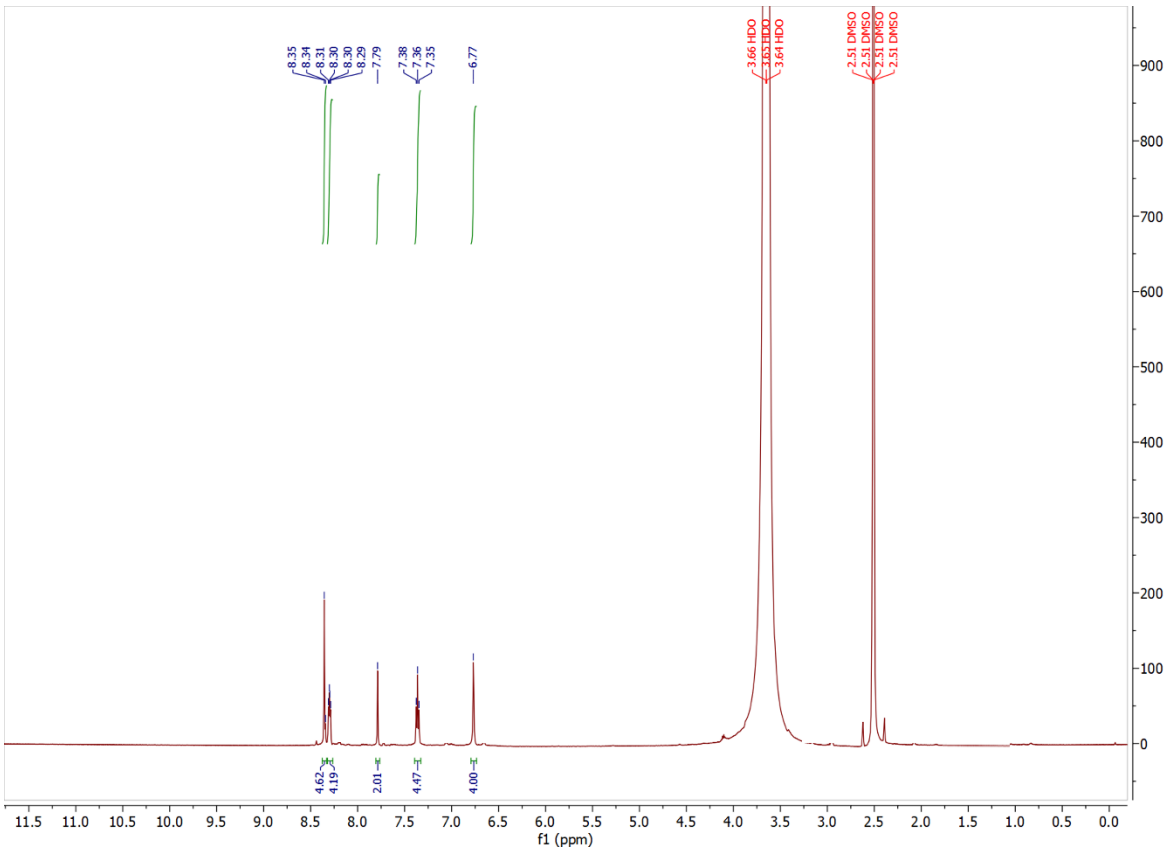

^{13}C-NMR Spectrum (151 MHz, DMSO-d_6) of Compound 3P

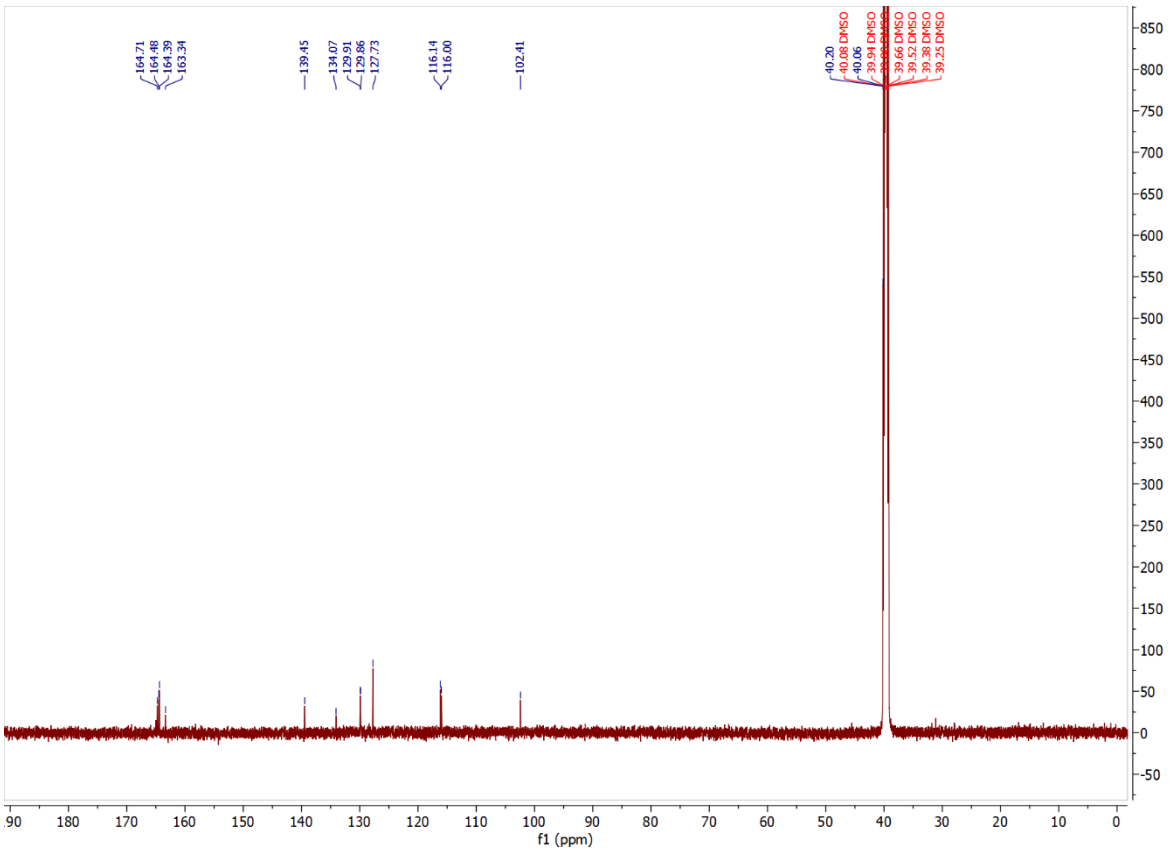

DEPT NMR Spectrum of Compound 3P

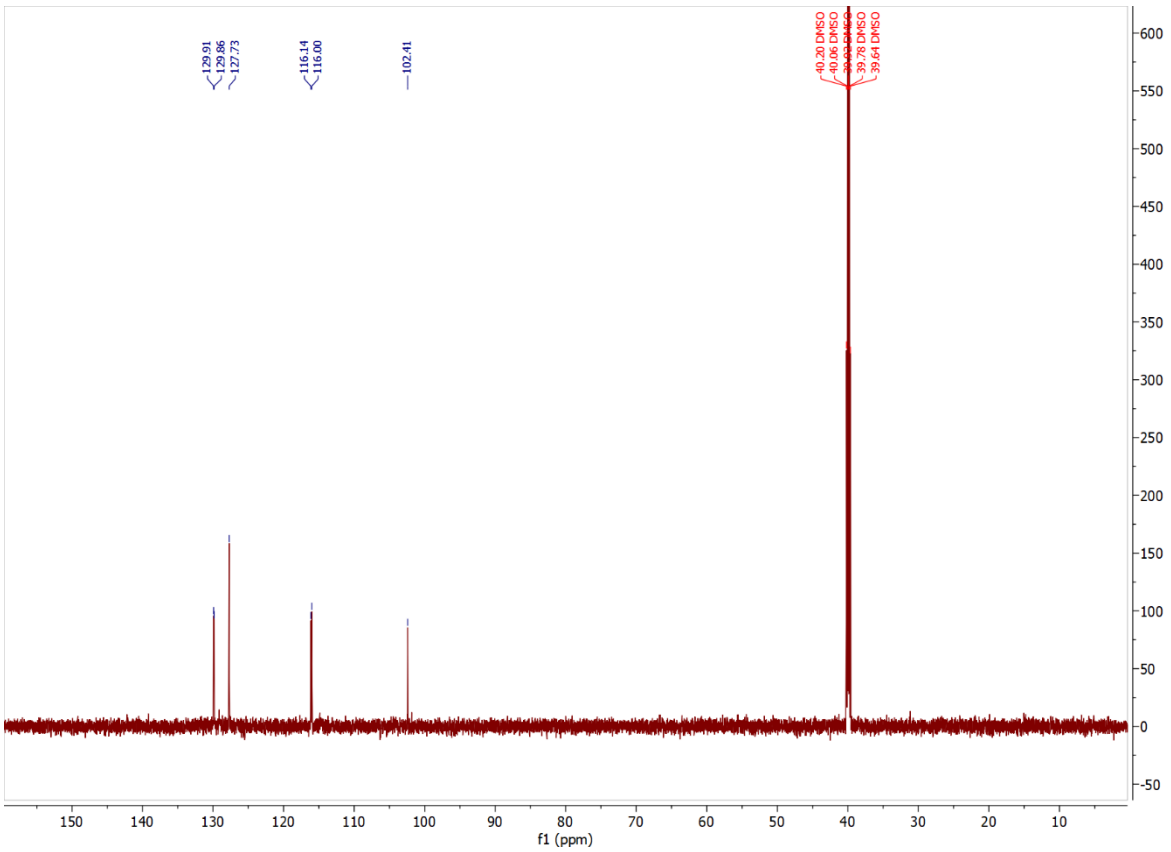

^{1}H-NMR Spectrum (600 MHz, DMSO-d_6) of Compound 4P

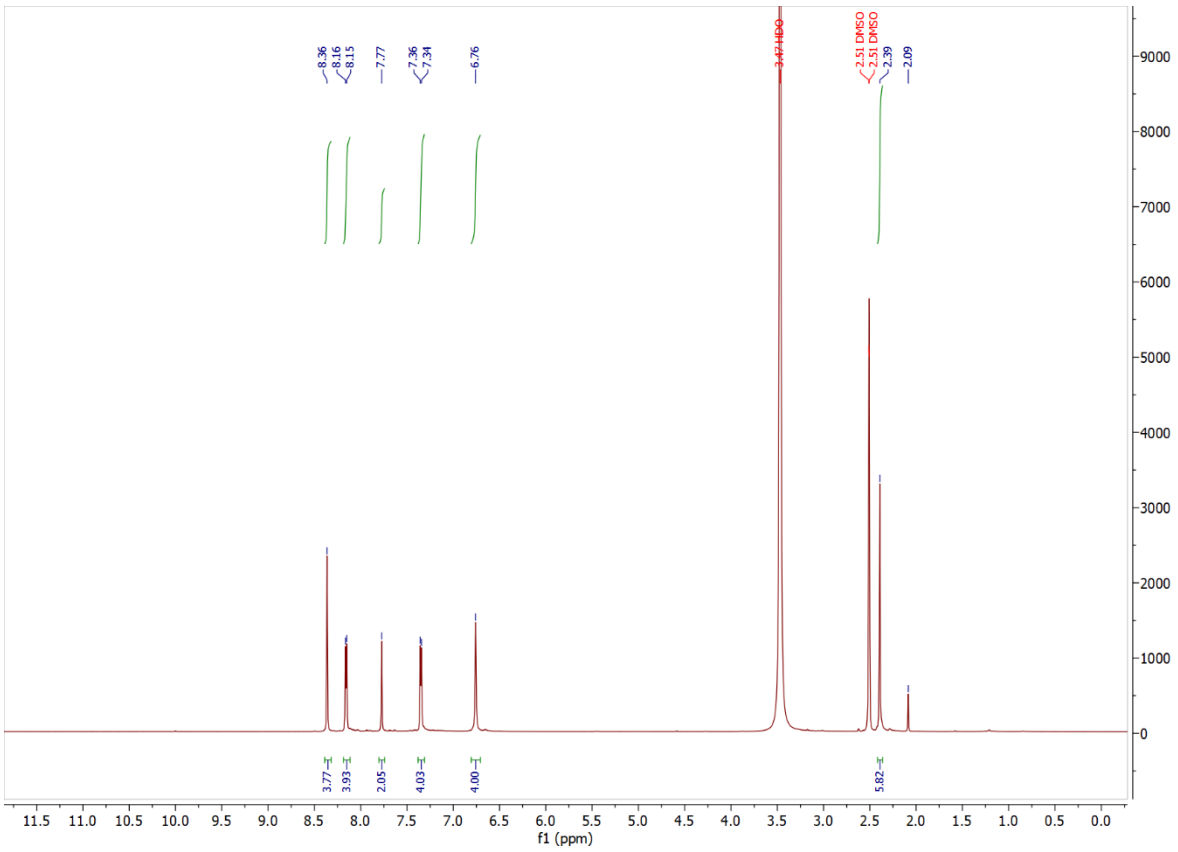

^{13}C-NMR Spectrum (151 MHz, DMSO-d_6) of Compound 4P

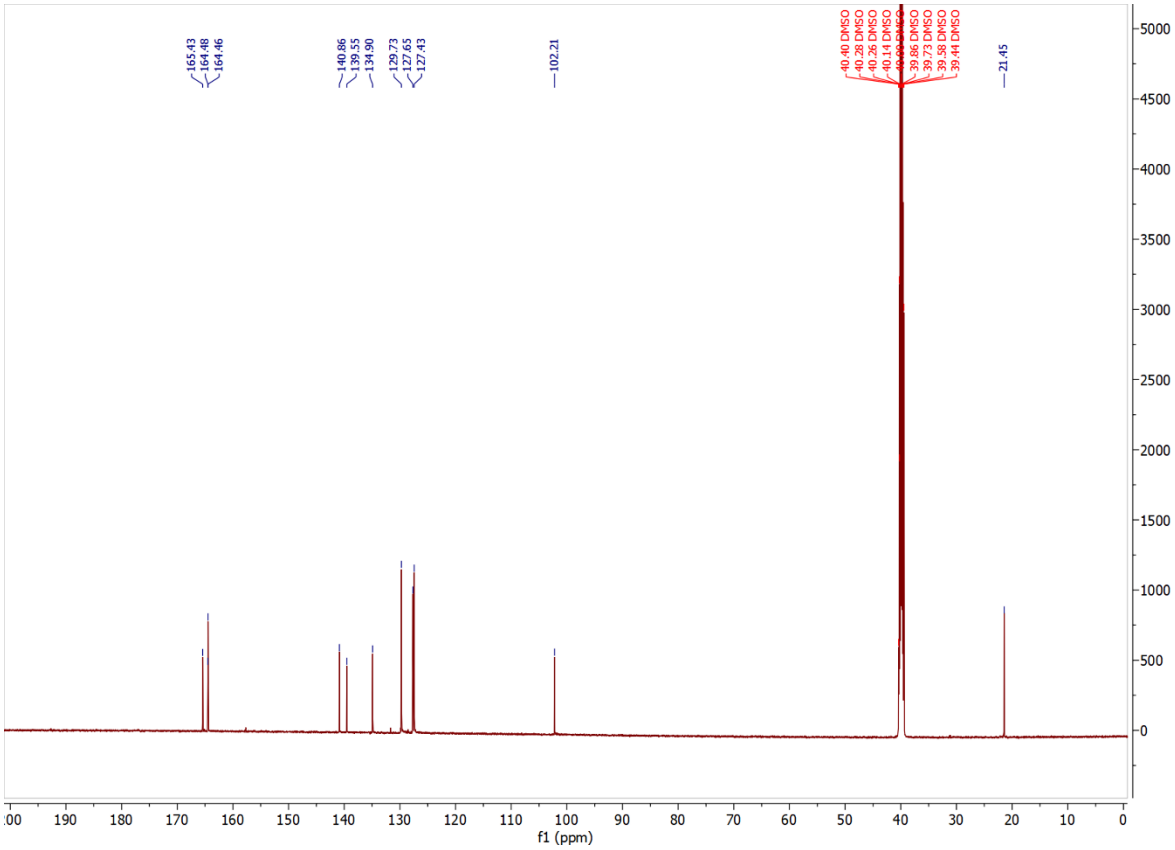

DEPT NMR Spectrum of Compound 4P

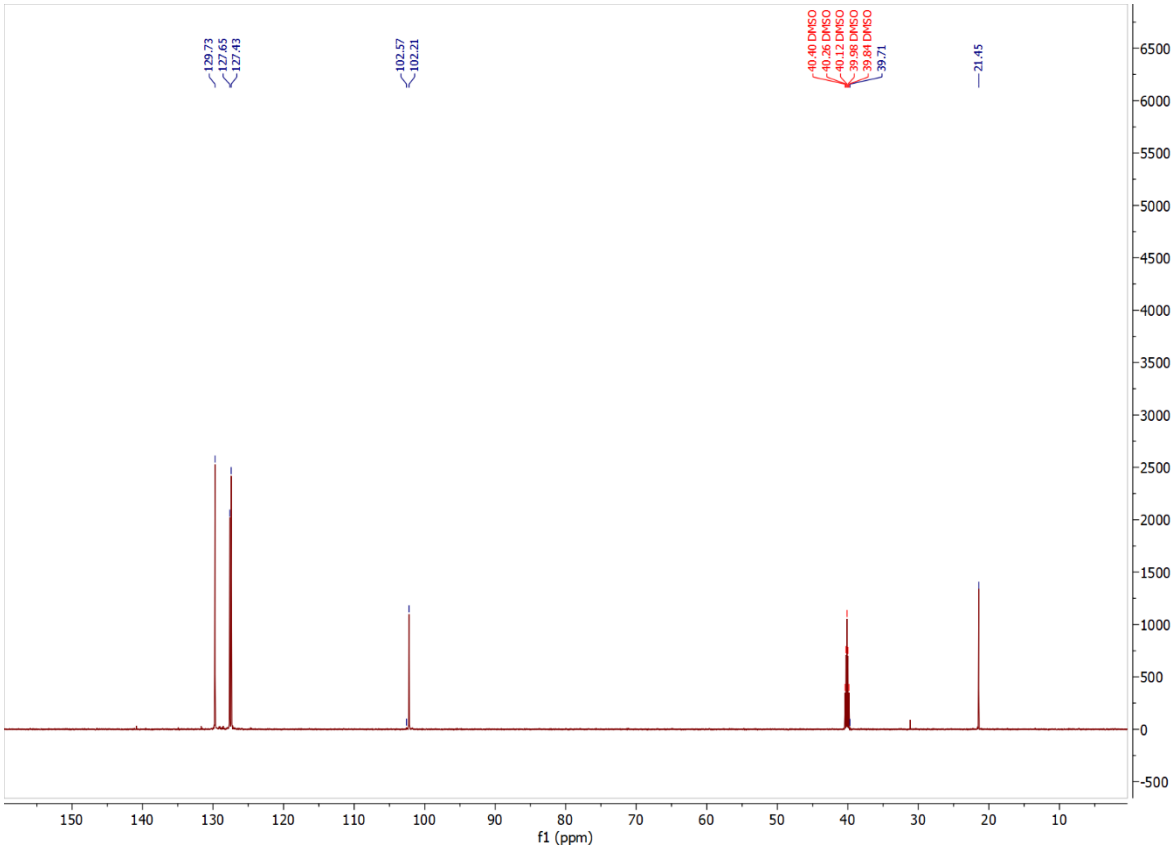

^{1}H-NMR Spectrum (600 MHz, DMSO-d_6) of Compound 5P

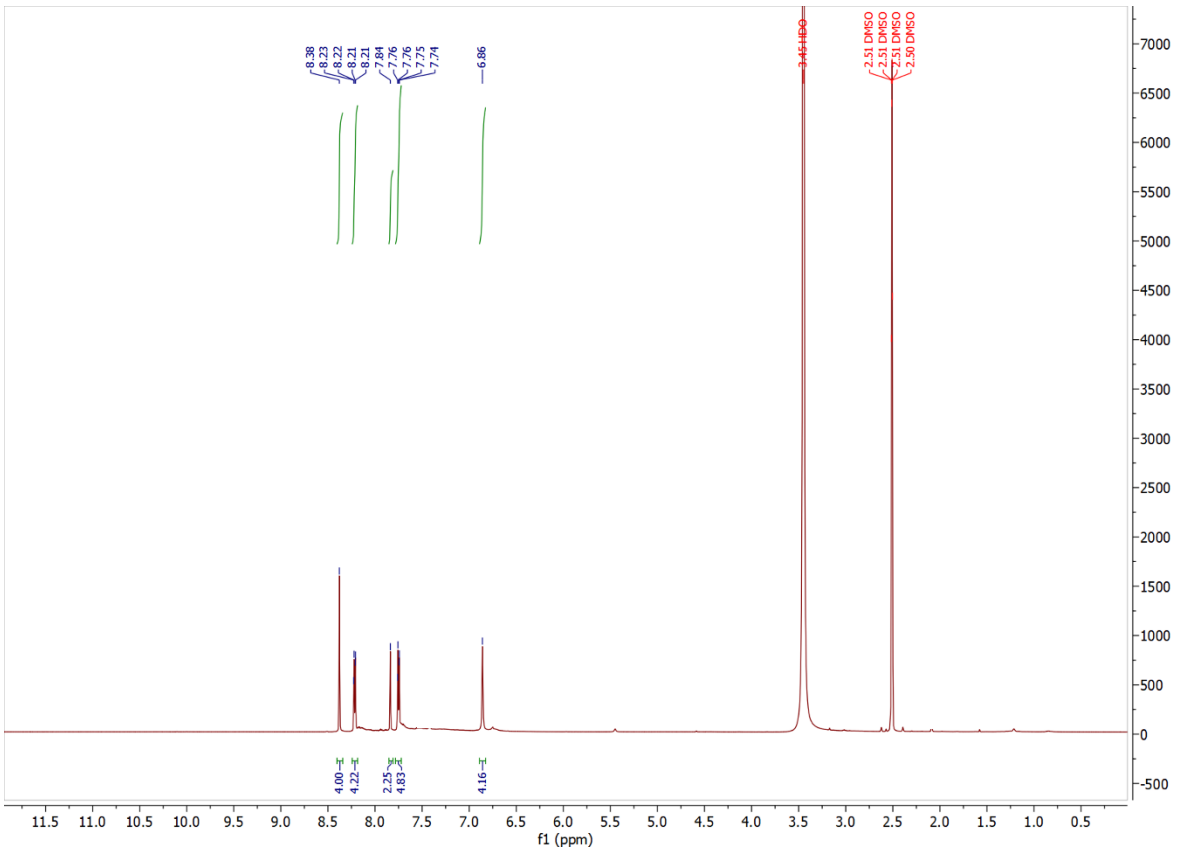

^{13}C-NMR Spectrum (151 MHz, DMSO-d_6) of Compound 5P

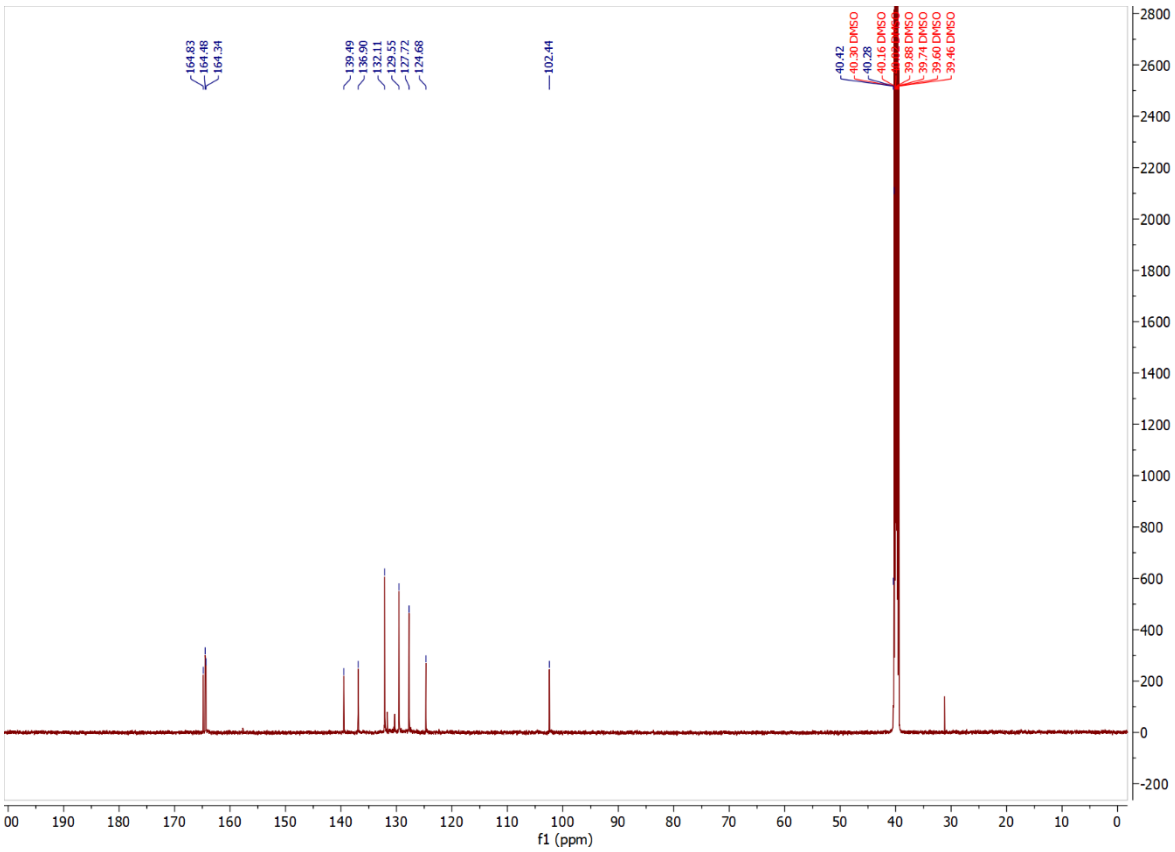

DEPT NMR Spectrum of Compound 5P

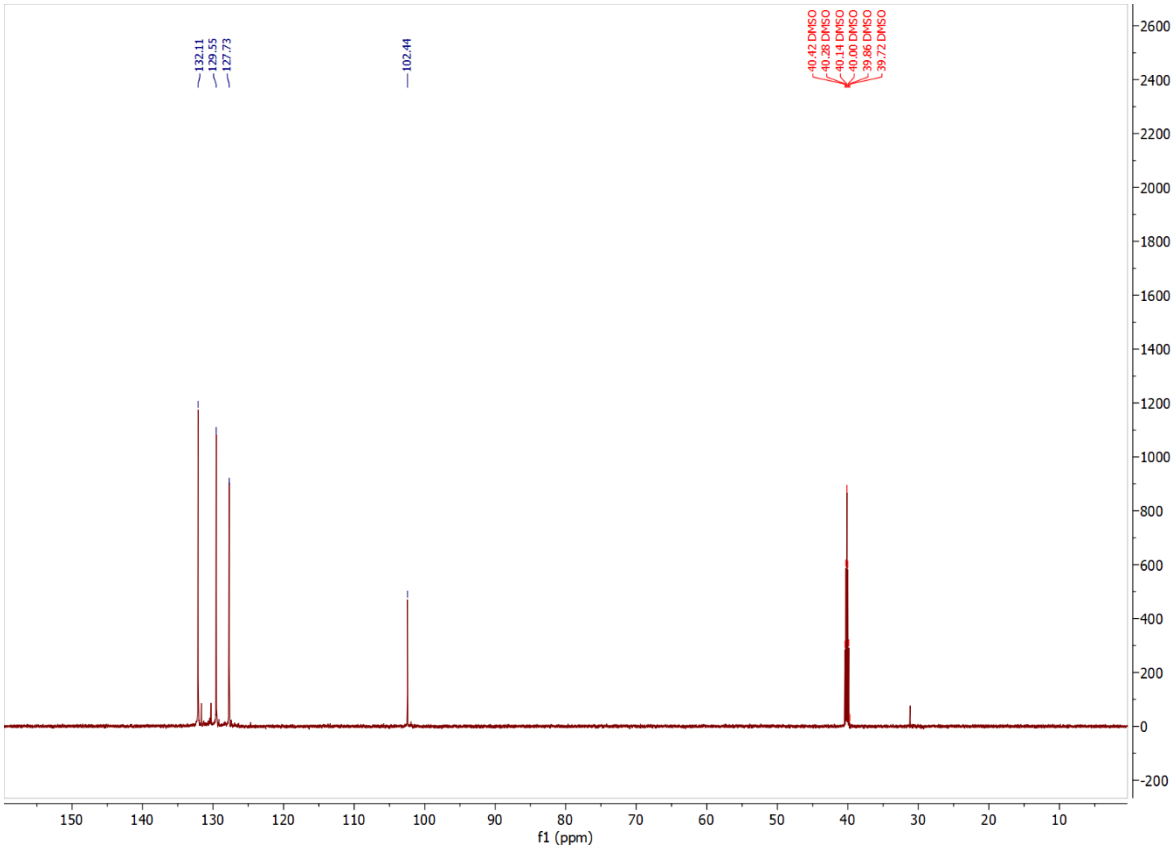

^{1}H-NMR Spectrum (600 MHz, DMSO-d_6) of Compound 6P

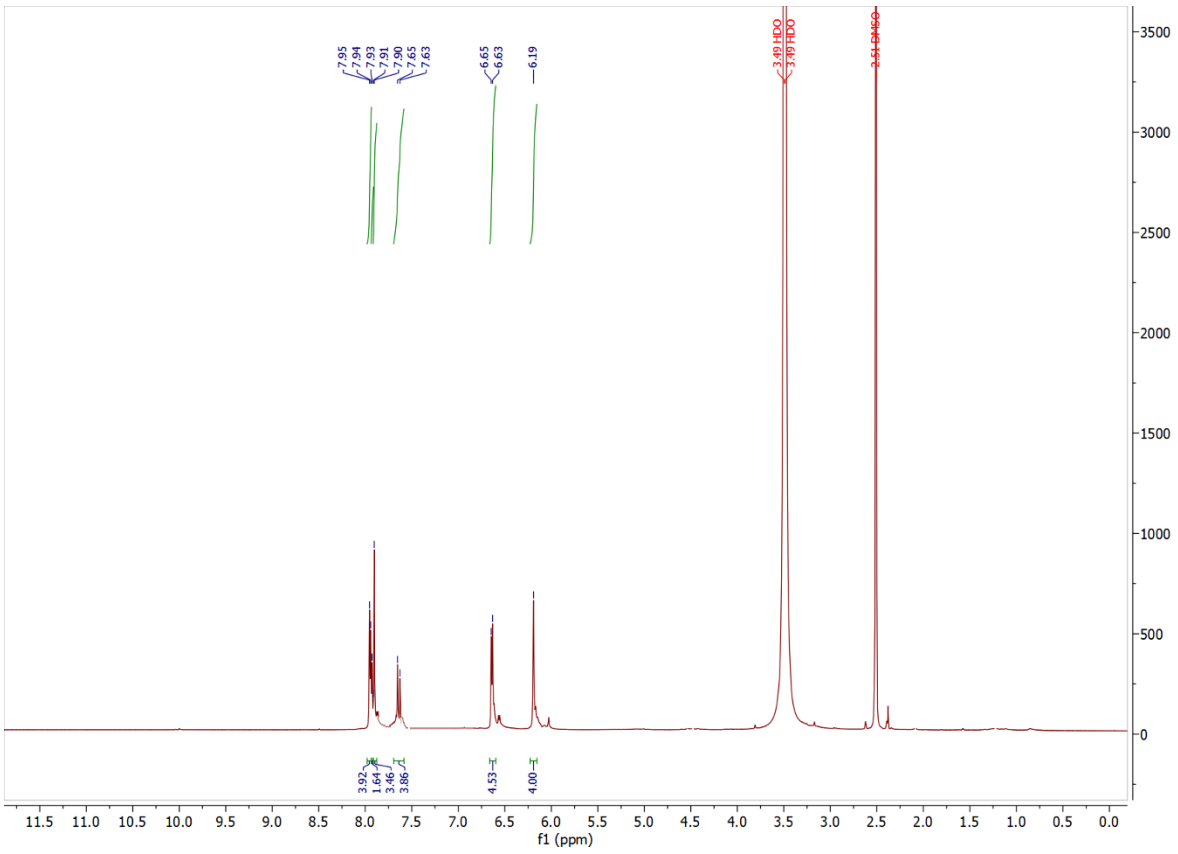

^{13}C-NMR Spectrum (151 MHz, DMSO-d_6) of Compound 6P

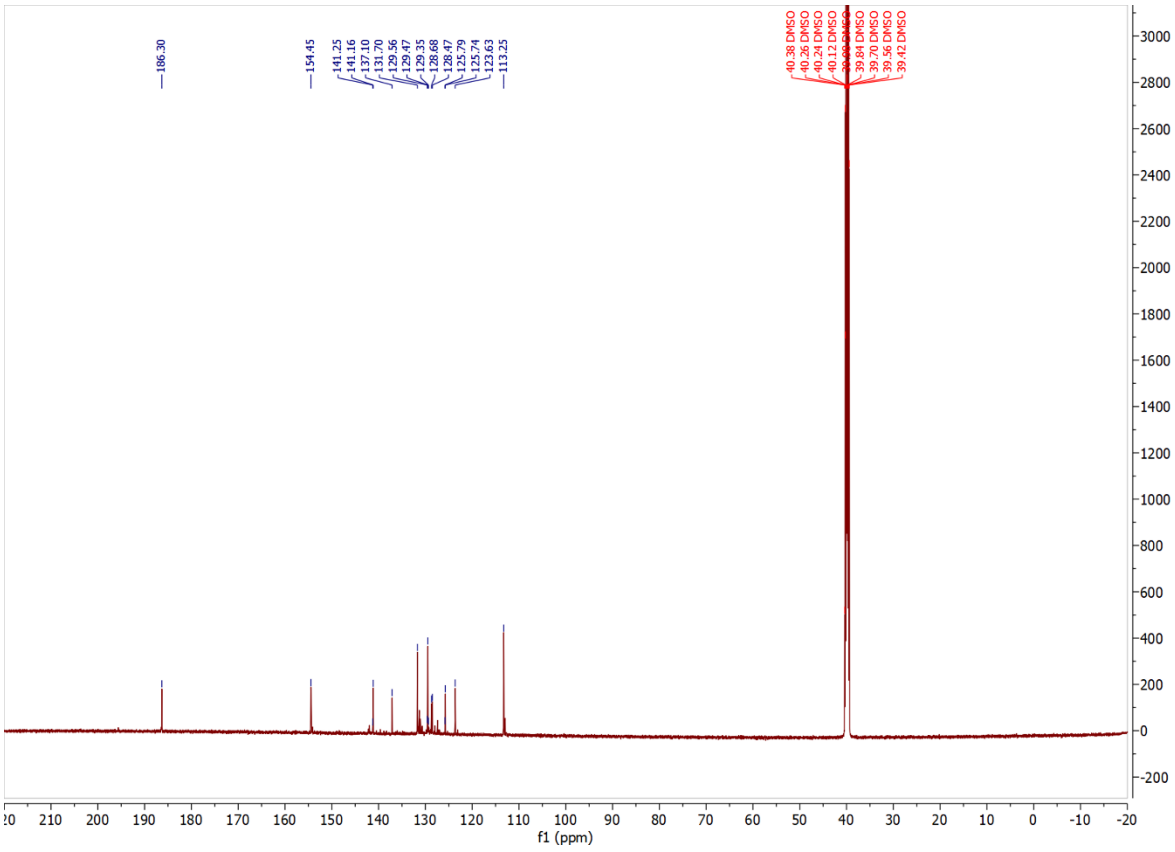

DEPT NMR Spectrum of Compound 6P

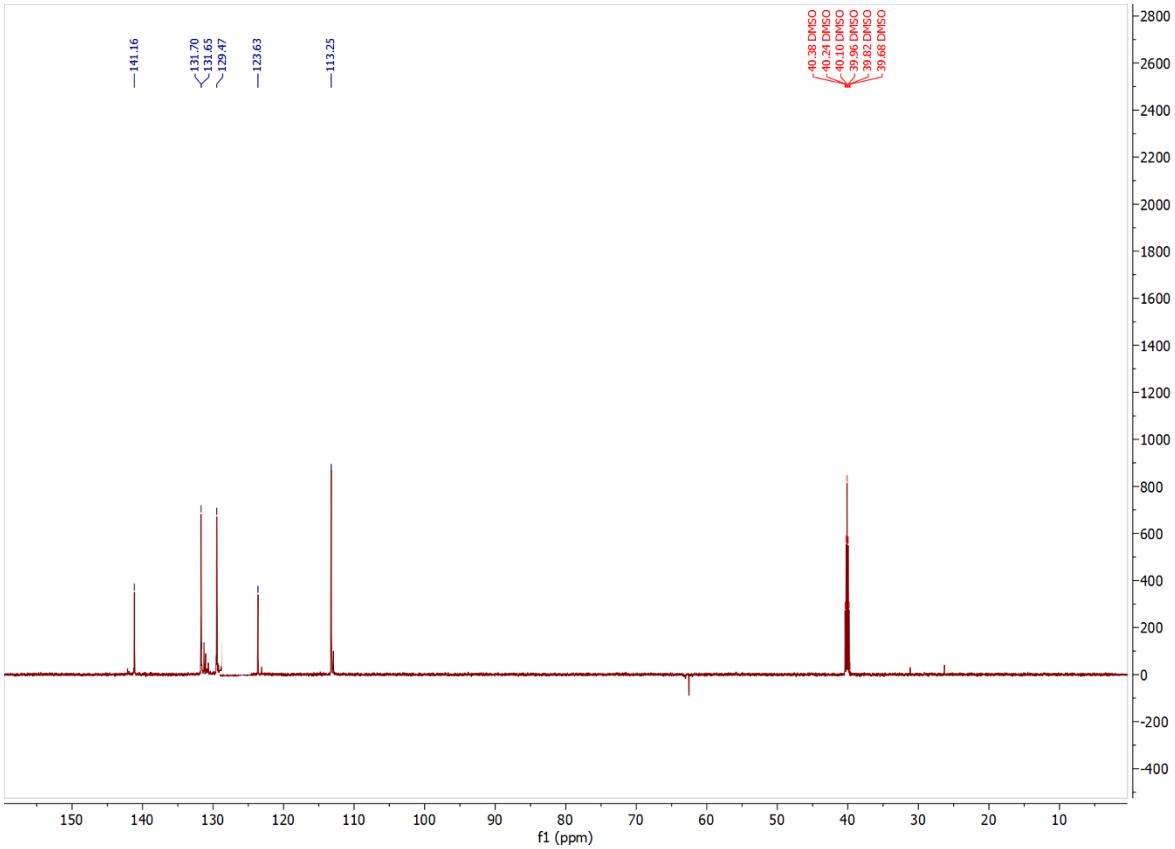

^{1}H-NMR Spectrum (600 MHz, DMSO-d_6) of Compound 7P

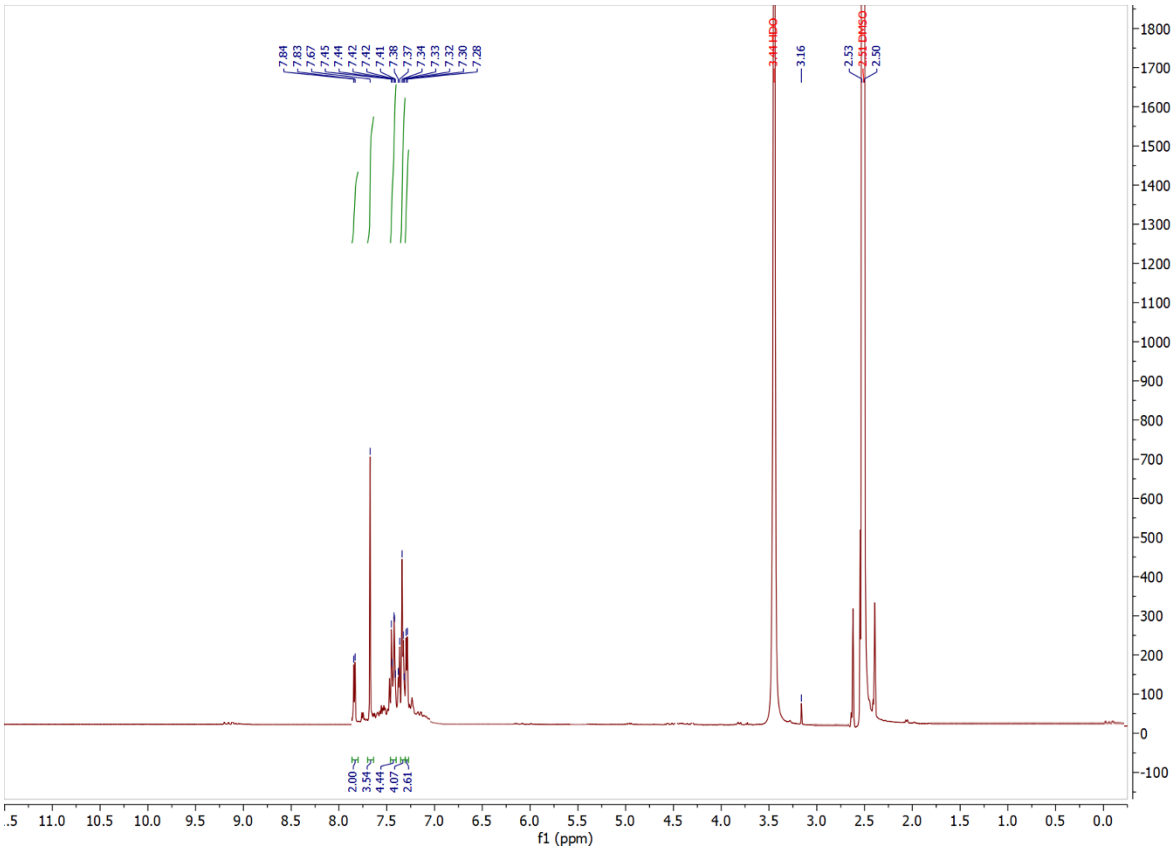

^{13}C-NMR Spectrum (151 MHz, DMSO-d_6) of Compound 7P

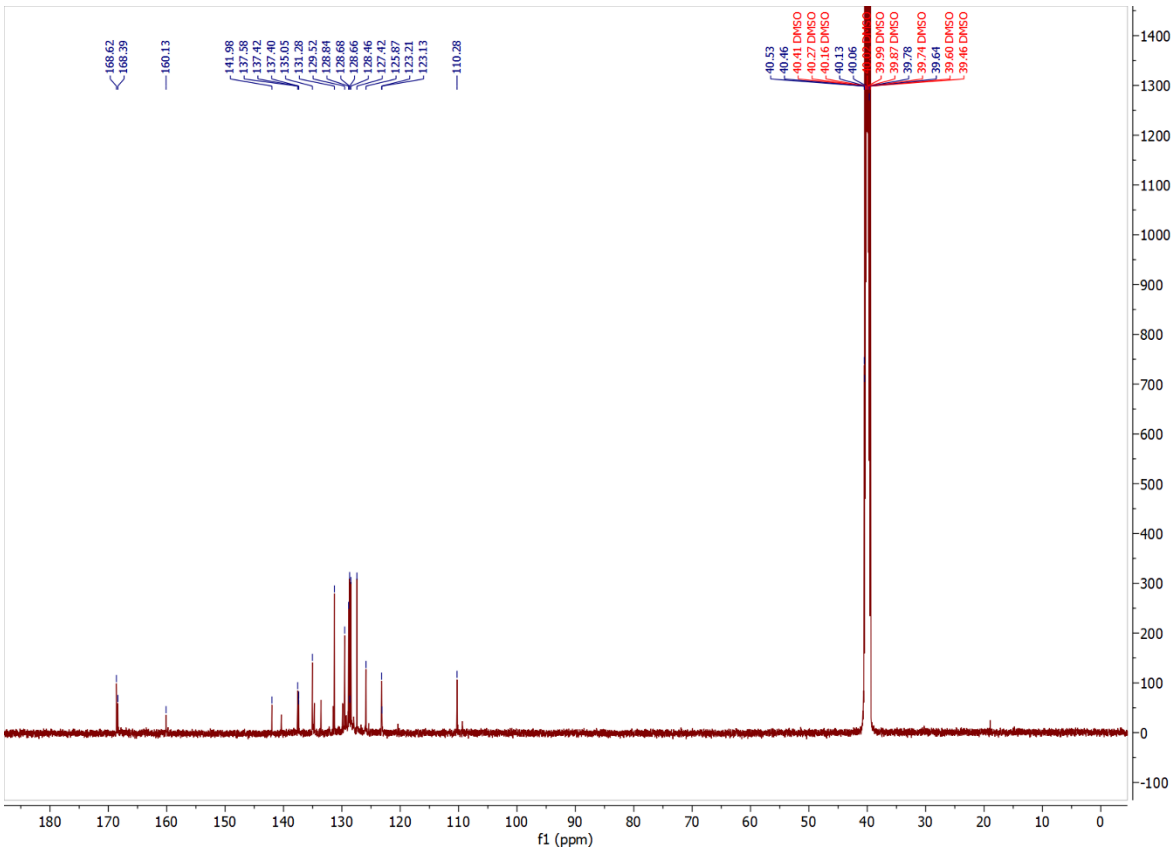

DEPT NMR Spectrum of Compound 7P

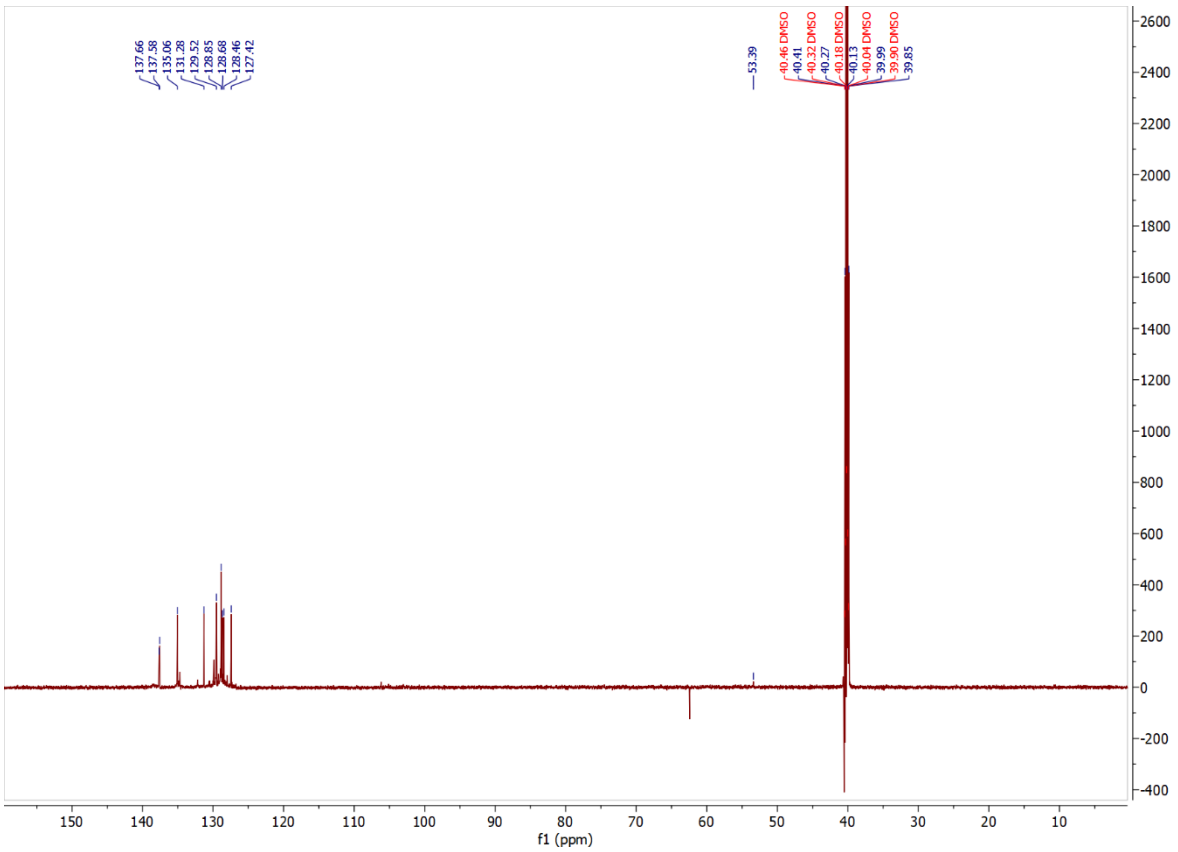

^{1}H-NMR Spectrum (600 MHz, DMSO-d_6) of Compound 8P

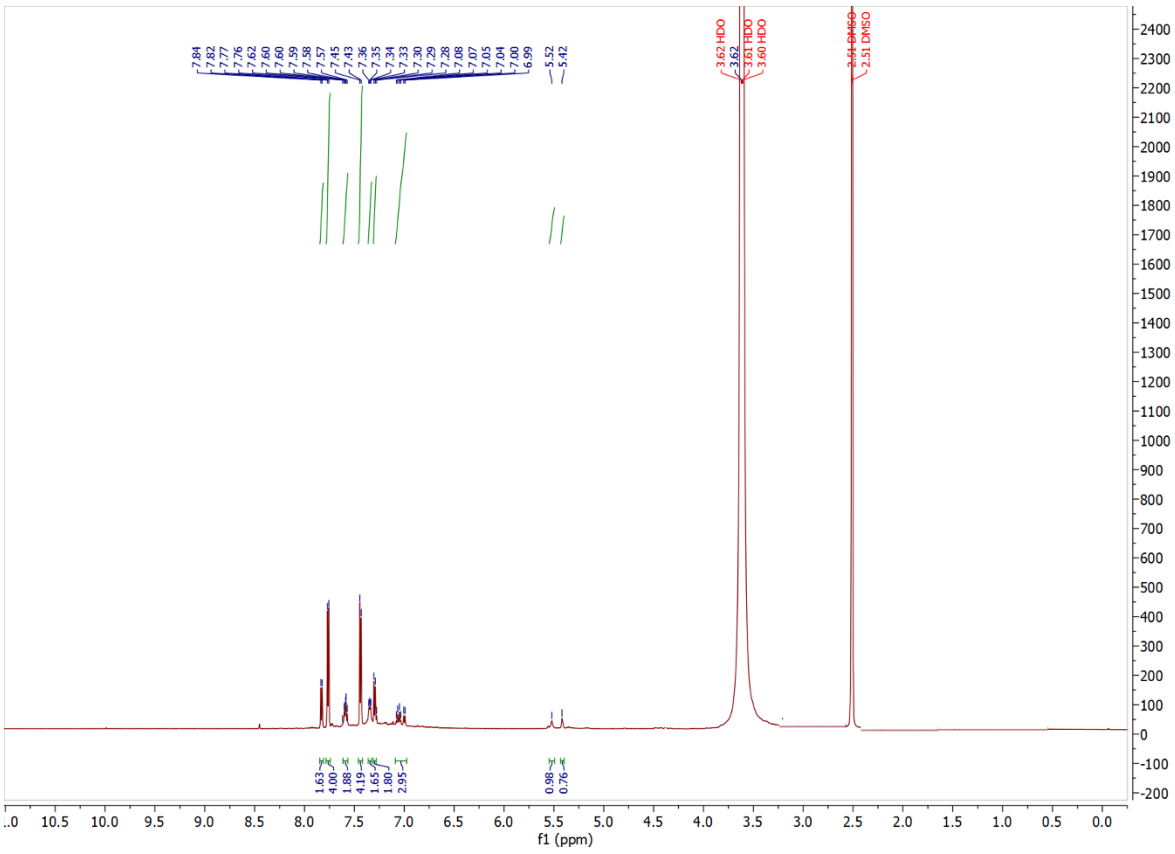

^{13}C-NMR Spectrum (151 MHz, DMSO-d_6) of Compound 8P

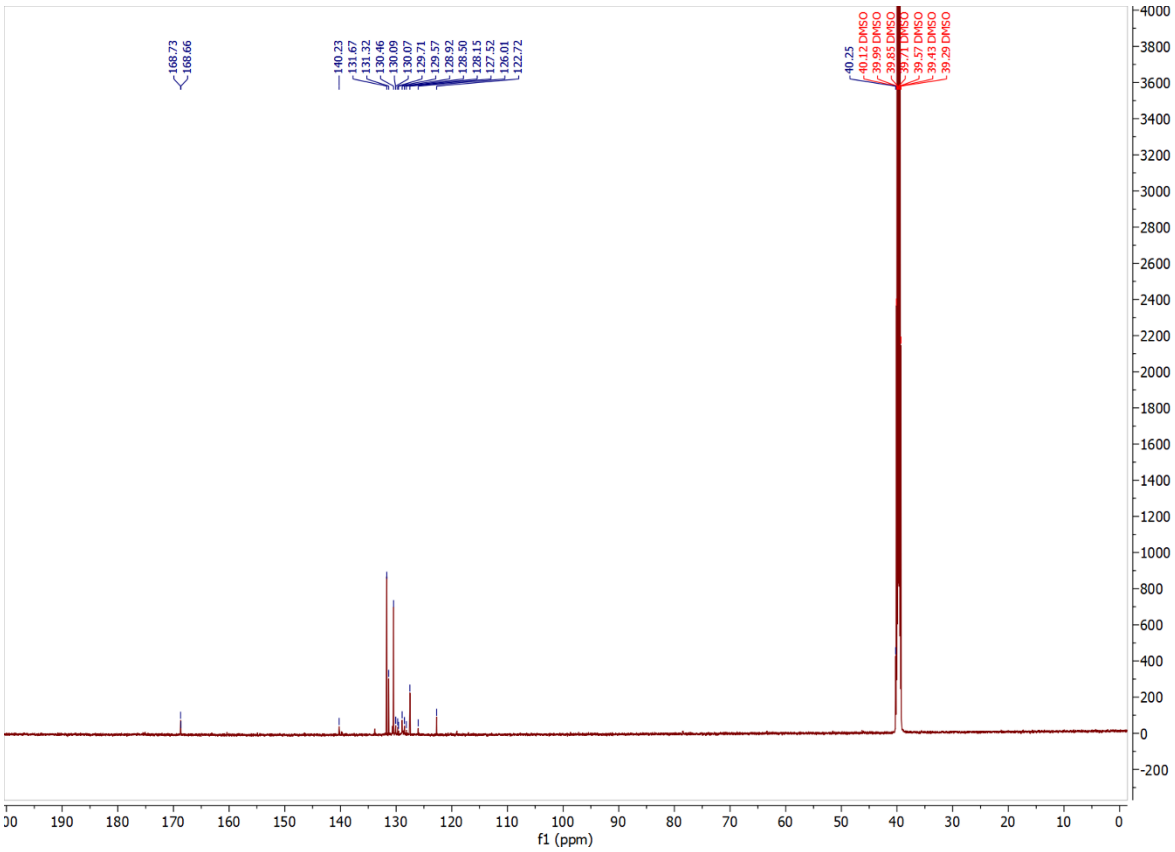

DEPT NMR Spectrum of Compound 8P